Proceedings World Geothermal Congress 2026
Calgary, Canada, June 8 – 11, 2026

Conceptual Model of Geothermal Potential in Northeastern Morocco: Approach Based on Geophysical, Geochemical, and Structural Analysis

Mohammed BOUMEHDI [1*], Nour Eddine BERKAT[1], Alae BARKAOUI[2] , Yassine ZARHLOULE[2],Júlio CARNEIRO[3], Mohammed Magoua[1], Lahsen ACHKOUCH[1] ,Anwar AIN TAGZALT[1],Doha DCHAR[1],Othman SADKI[1],Mustapha CHAIB[1]

National Office of Hydrocarbons and Mines, 5, Avenue Moulay Hassan – Rabat, BP. 99, Morocco [1*], Faculty of sciences, University of Mohamed I, Oujda 6000, Morocco [2]; Faculty of sciences Ben M'sick, Université Hassan II, Casablanca, Morocco [2], ICT – Instituto de Ciências da Terra, Universidade de Évora, Évora, Portugal[3]

*Corresponding author: Mohammed BOUMEHDI, Email: boumehdi@onhym.com

Keywords: Geothermal systems, Northeastern Morocco, heat flow density, geothermal gradient, conceptual model, geophysics, hydrogeochemistry, structural analysis.

ABSTRACT

The northeastern region of Morocco, considered the most promising geothermal province in the country, is located along the SW-NE trend known as the Moroccan Hot Line (MHL). This area is marked by recent volcanic activity, a thinned crust and lithosphere, and geothermal gradients and heat flow exceeding 40 °C/km and 110 mW/m^2. It is also characterized by numerous hot springs, many of which exhibit significant CO_2 emissions, indicating deep geothermal activity. This study develops a conceptual model of geothermal potential in this region, based on previous geothermal exploration conducted by the National Office of Hydrocarbons and Mines (ONHYM), including temperature measurements, geochemical and gas sampling. The model has been further refined by integrating structural analyses derived from satellite gravity data and magnetic spectral analysis, enhancing the delineation of geothermal anomalies and providing insights into the deep-seated structures that control the geothermal system. The study identifies key geothermal zones (Berkane/Fezouane, Gourougou/Driouch, and Arekman/Ras El Ma) as the most promising for both electricity generation and direct uses. These zones exhibit significant geothermal anomalies and are closely associated with deep structural features revealed by these geophysical analyses. This updated conceptual model offers a robust framework for future exploration and sustainable development of geothermal resources in Northeastern Morocco, contributing to the country's renewable energy goals.

1 INTRODUCTION

Located in the northwestern part of the African plate, Morocco is a site of lithospheric shortening related to the Africa-Europe convergence. Within this geodynamic framework, Northeastern Morocco is recognized as the country's most promising geothermal province. The region is situated along the major SW-NE axis known as the Morocco Hot Line (MHL), characterized by crustal and lithospheric thinning, as well as recent volcanic activity (Neogene-Quaternary) (de Lamotte et al., 2009; Rimi et al., 2012).

The abundance of hot springs and recent volcanism has prompted numerous geothermal studies over several decades (e.g.,(Alsac Et Al., 1969; Barkaoui Et Al., 2017; Haffou Et Al., 2024; Ouzzaouit Et Al., 2023; Rimi Et Al., 2012; Rimi & Lucazeau, 1987; Zarhloule Et Al., 2007). Regional analysis from the Eastern Rif and Middle Atlas toward Northwestern Algeria indicates a heat flow density ranging from 80 to 110 mW/m^2 (Zarhloule et al., 2015)l and high geothermal gradient values reaching 50 °C/km (Rimi, 1999; Zarhloule, 2004).

In the sedimentary basins of this region, the deep circulation of geothermal fluids is facilitated by complex fracture systems (Rimi, 1999; Zarhloule et al., 2007). The dolomitic/limestone Liassic aquifer is considered the prominent geothermal reservoir in the eastern part of the country. More than 25 hot springs are documented in this aquifer, with surface temperatures ranging from 26 to 54 °C and flow rates occasionally exceeding 40 L/s. Subsurface data confirms this thermal intensity; for instance, borehole 1624/7 reveals a temperature of 50 °C at 470 m depth. Notably, the geothermal gradient in this well increases sharply below 300 m, rising from 29 to 127 °C/km, with an estimated bottom-hole temperature of approximately 120 °C (Barkaoui et al., 2014, 2017).

Recent investigations have diversified the methodological approaches to better constrain this potential. (Boumehdi et al., 2025) recently confirmed the area's elevated potential through spectral analysis of magnetic data, providing estimates of heat flow and geothermal gradients derived from the Curie Point Depth.

Complementing this, (Ouzzaouit et al., 2023) applied machine learning algorithms (including Multi-Layer Perceptron and Support Vector Regression) to model geothermal flow. By integrating multi-source data such as Bouguer gravity, aero-magnetic fields, and fracture density their predictive model highlighted high geothermal flow anomalies in Northeastern Morocco, attributing them to deep magmatic intrusions linked to the regional geodynamic context.

Despite these extensive assessments and the accumulation of high-quality data, a synthesis integrating these recent geophysical findings into a coherent structural model is still required to fully understand the heat transfer mechanisms. The present paper aims to consolidate these previous exploration results to develop an updated conceptual model of the Northeastern Morocco geothermal system. This work focuses on defining the structural controls of the reservoir to provide a robust framework for future exploitation strategies.

2 . GEOGRAPHIC AND GEOLOGICAL FRAMEWORKS OF THE STUDY AREA

The general geological context of Northeastern Morocco is fundamentally governed by its strategic position within the convergence belt between the African and Eurasian plates in the Western Mediterranean. This major tectonic interaction drives a complex regional stress regime, characterized by a predominant NNW-SSE compressive orientation, and significant seismicity, particularly along the Iberia-Africa plate boundary(Platt et al., 2013; van Hinsbergen et al., 2014).The region is situated along a major NE-SW trend extending from the Anti-Atlas to the Eastern Betics, known as the Morocco Hot Line (MHL)(de Lamotte et al., 2009; Missenard et al., 2006). This zone is marked by active lithospheric extension, corroborated by deep geophysical investigations. Receiver function analysis and seismic tomography reveal a sharp crustal thinning, transitioning from 35–44 km in the northwestern domain to 22–30 km beneath the study area (Díaz et al., 2016; Fullea et al., 2006; Mancilla & Diaz, 2015). This crustal geometry is accompanied by a shallow Lithosphere-Asthenosphere Boundary (LAB) estimated at less than 100 km depth, and a distinct low-velocity P-wave anomaly in the upper mantle, suggesting asthenospheric upwelling [2].These deep processes are reflected in the geophysical signatures of the region. Gravity data show a regional Bouguer anomaly gradient increasing from a negative axis of -100 mGal in the south (High Plateaus) to +40 mGal in the north (Nador region), mirroring the northward crustal thinning (Fullea et al., 2006, 2007; Gil et al., 2014; Li et al., 2021). Furthermore, magnetic surveys highlight major E-W trending anomalies, notably coinciding with the Gourougou volcanic complex and the Kariat Arekman zone, indicating the presence of shallow magmatic intrusions controlled by deep NE-SW lineaments (Boumehdi et al., 2025; El Bakkali et al., 1998).Structurally, the region acts as a transition zone between the Alpine Rif belt to the north and the Atlasic and Saharan domains to the south. It is characterized by brittle tectonics and a dense fracture network, largely influenced by the active Trans-Alboran fault system, which plays a primordial role in hydrothermal fluid circulation (Jacobshagen, 1992). The main morphostructural units include the Eastern Rif, the Beni Snassen massif (a major carbonate horst), the Taourirt-Oujda Corridor, and the High Plateaus .The lithostratigraphy is highly diversified. The Paleozoic basement, composed of schists and Variscan granitoids (such as those at Aouli or Beni Snassen), is overlain by a thick sedimentary sequence. The Mesozoic is of particular importance, specifically the Liassic (Lower Jurassic), which consists of fractured limestones and dolomites that form the primary deep geothermal aquifers. These carbonate reservoirs are often confined by overlying impermeable formations. The Cenozoic is represented by Plio-Quaternary sedimentary deposits filling vast subsiding depressions, such as the Triffa plain, often interstratified with volcanic products. Widespread recent volcanism (14.6 to 0.3 Ma) is a defining characteristic of the area. This Neogene-Quaternary activity exhibits a geochemical transition from calc-alkaline to alkaline series, serving as a key indicator of the high terrestrial heat flow. The combination of these factors a crust affected by extension, deep fault structures, continuous magmatic activity, and fractured carbonate reservoirs endows Northeastern Morocco with a geothermal gradient significantly above the regional average, justifying the assessment of its high-enthalpy resource potential.

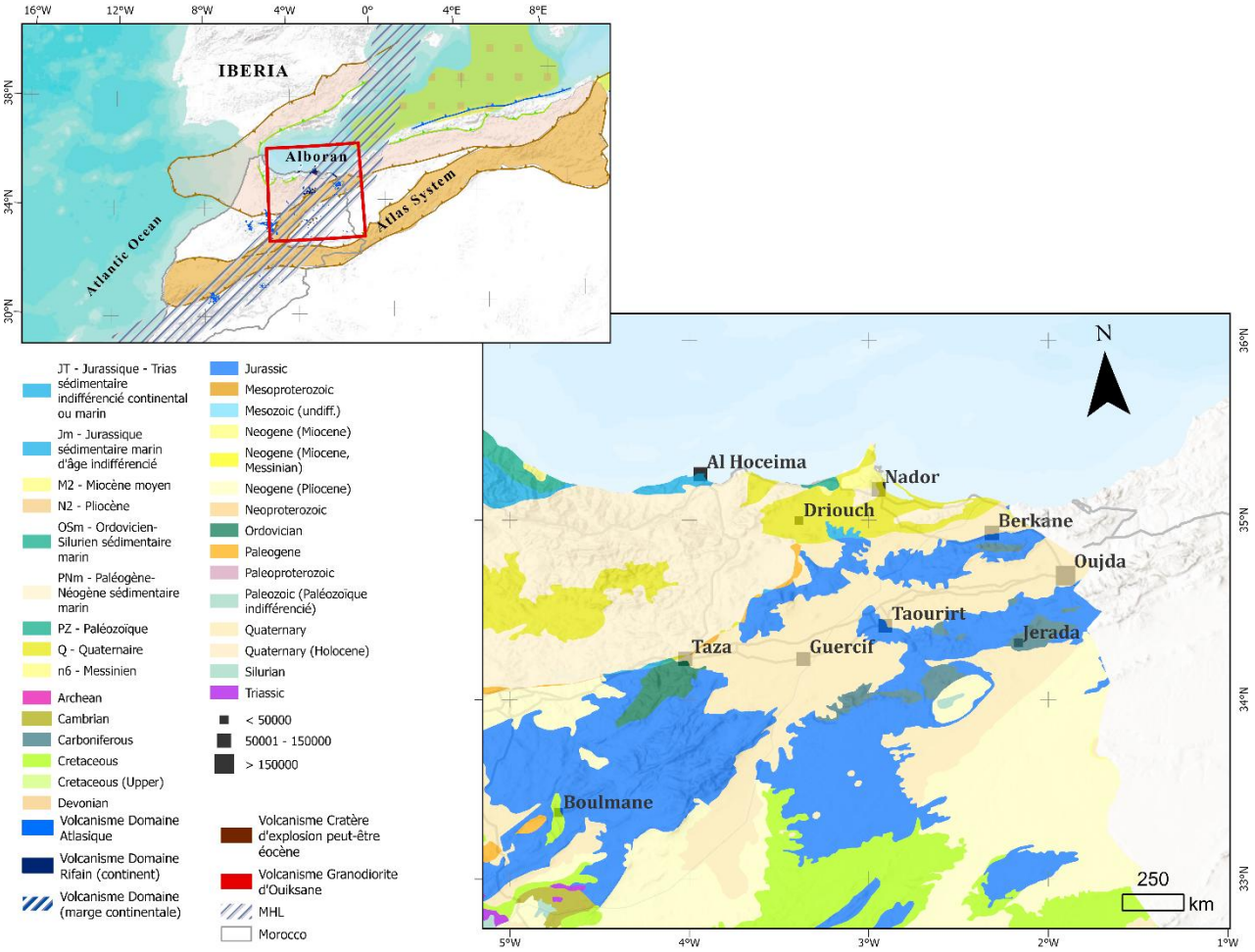


Figure 1. Geographical framework and simplified geological map of the study area showing the main morpho-structural units.

3 DATA AND METHODS

To develop a robust conceptual model of the Northeastern Morocco geothermal system, a multi-disciplinary approach was adopted, integrating geochemical, thermal, and geophysical datasets. The methodology combines direct field measurements with remote sensing analysis to constrain the heat source, reservoir characteristics, and structural controls.

3.1 Geochemical and Isotopic Data

A comprehensive hydrogeochemical campaign was conducted to characterize the fluids and estimate reservoir temperatures. The dataset includes 128 groundwater and gas samples collected from 27 representative sites, including thermal springs and boreholes.

3.1.1 Physico-chemical Composition of Waters

To determine the physico-chemical characteristics of the geothermal fluids, unstable parameters including temperature, pH, electrical conductivity (EC), redox potential (Eh), and alkalinity were measured in situ immediately upon sampling using portable digital meters. Water samples were collected in polyethylene bottles; samples destined for cation analysis were filtered through 0.45 µm membranes and acidified with nitric acid (HNO_3) to prevent precipitation, while anions were analyzed from non-acidified samples. Major ions (Na^+, K^+, Ca^{2+}, Mg^{2+}, Cl^-, SO_4^{2-}, HCO_3^-) were determined using Ion Chromatography (IC) and Titration, and trace elements were analyzed via Inductively Coupled Plasma Mass Spectrometry (ICP-MS). The hydrochemical facies and mineralization processes were subsequently defined using Piper trilinear diagrams and ionic correlation plots.

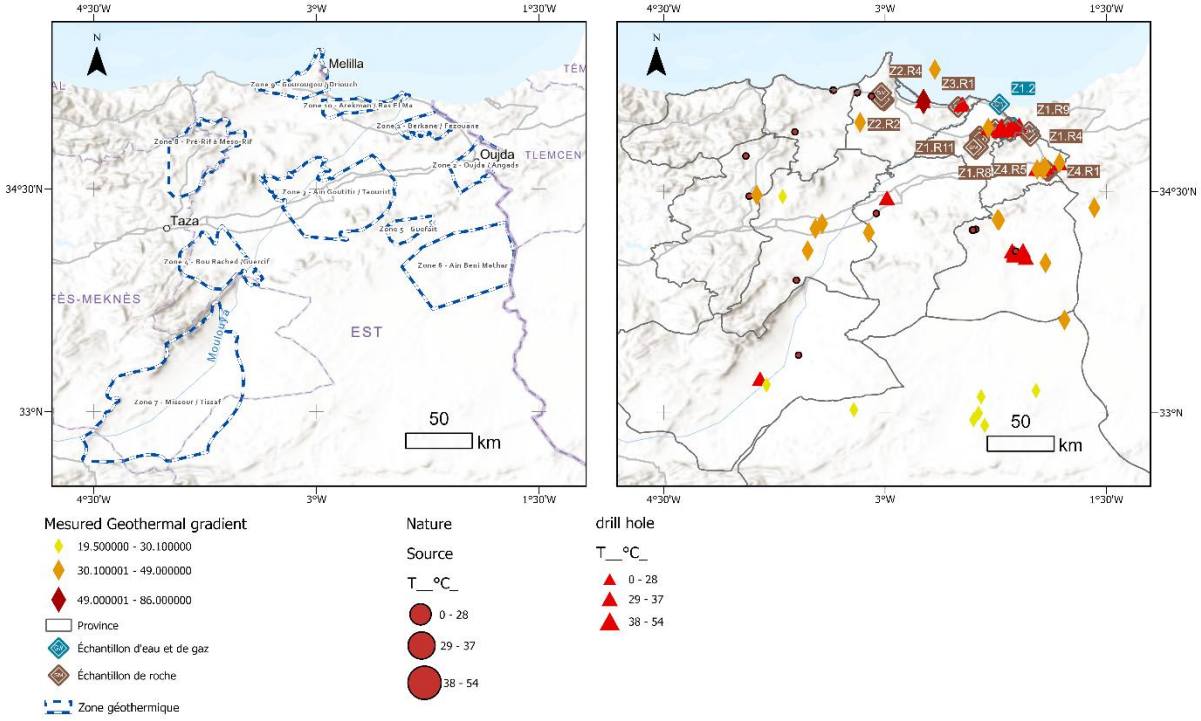


Figure 2. (Left) Map of the identified geothermal zones; (Right) Location and number of samples per zone with measured geothermal gradient values.

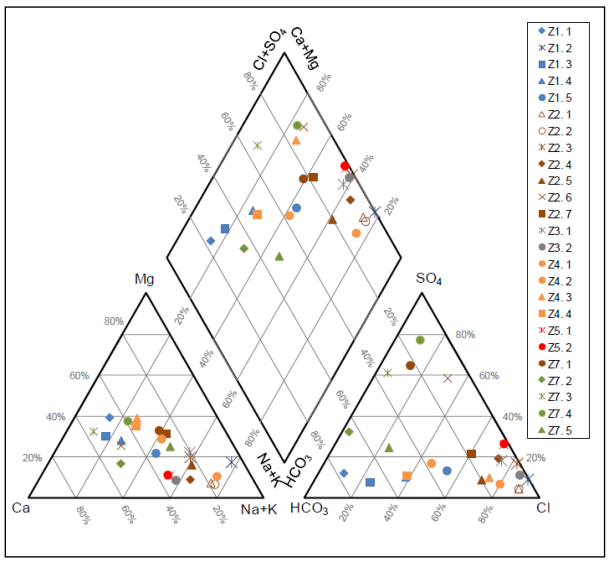


Figure 3. Representation of the hydrochemical facies of Northeastern Morocco waters on a Piper diagram.

The hydrochemical analysis reveals that the majority of the sampled waters belong to the Ca-HCO3, Na-Cl, or Ca-Na-Cl facies. This distribution distinguishes two main hydrogeological behaviors (Figure3):

- Pre-Rif to Meso-Rif Zone: Characterized by deep circulation associated with Ca-HCO3 facies, while shallower circulation pathways exhibit Ca-SO4 characteristics.
- Berkane/Fezouane Zone: Characterized by waters ranging from calcium-bicarbonate to calcium-chloride types.

The correlation between Sodium (Na+) and Chloride (Cl-) ions (in meq/L) is strong and follows the seawater dilution line (Figure 4). This indicates a significant contribution of marine salts, likely derived from either the evaporation of recharge water or circulation through evaporitic rocks (gypsum/halite). Consequently, the highest

concentrations of these ions are observed in the Gourougou/Driouch and Arekman/Ras El Ma zones (due to coastal proximity) and the Ain Goutitir/Taourirt zone (where the presence of Triassic evaporites is confirmed). In contrast, the Berkane/Fezouane zone exhibits significantly lower concentrations.

Exceptions to this trend are observed in the Pre-Rif to Meso-Rif zone, where higher Na+ concentrations are likely linked to the dissolution of Na-bearing minerals (silicate weathering), and in the Oujda/Angads zone (samples Z4.3 and Z4.6), which displays lower Na+ levels.

Furthermore, the lack of correlation between Na+ and HCO3 confirms that the mineralization process is primarily driven by the acquisition of marine salts (Na+Cl) rather than carbonate dissolution. Similarly, the relationship between Cl- and HCO3- shows complete independence, indicating distinct origins for these ions (Figure 5).

Finally, a Ca/Mg ratio close to 1:1 is observed in many samples, indicating a strong dependence on dolomitic reservoir rocks. However, this signature is absent in the waters of Ain Goutitir/Taourirt and specific samples from the Gourougou/Driouch, Arekman/Ras El Ma, and Pre-Rif zones, suggesting more complex lithological interactions in these sectors (Figure 6).

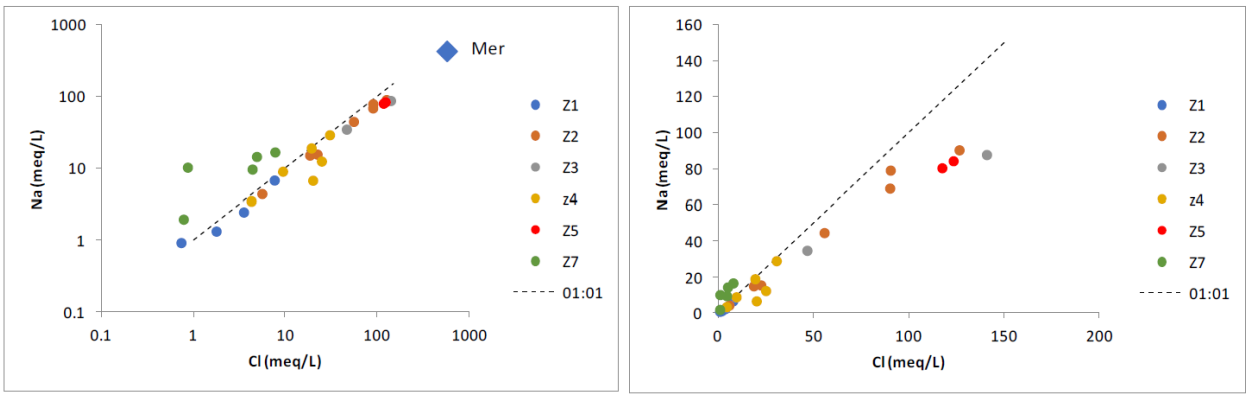


Figure 4 (Left) Relationship between chloride and sodium ions (meq/L) in sampled waters on a logarithmic scale, showing the composition of Mediterranean seawater; (Right) Relationship between chloride and sodium ions (meq/L) in sampled waters, with the 1:1 correlation line

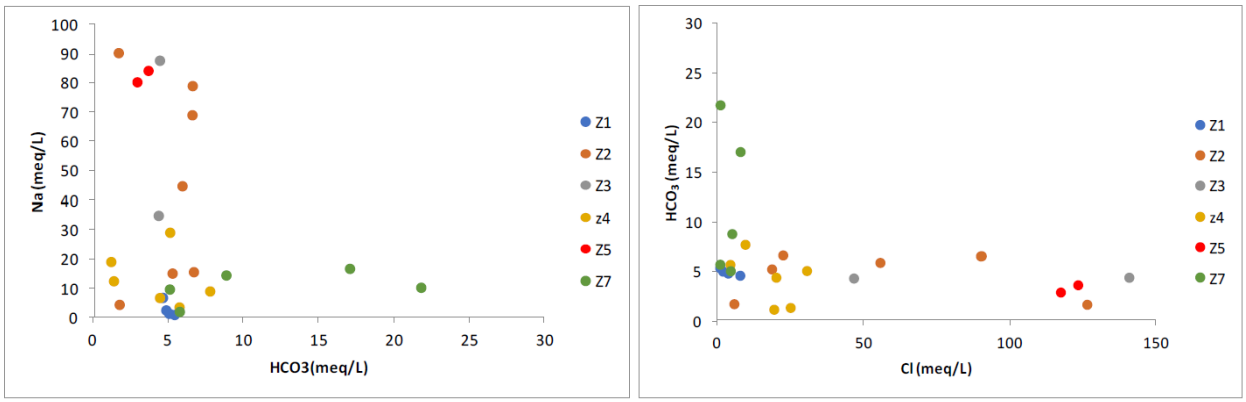


Figure 5. (Left) Plot of sodium versus bicarbonate concentrations; (Right) Plot of chloride versus bicarbonate concentrations in the analyzed water samples.

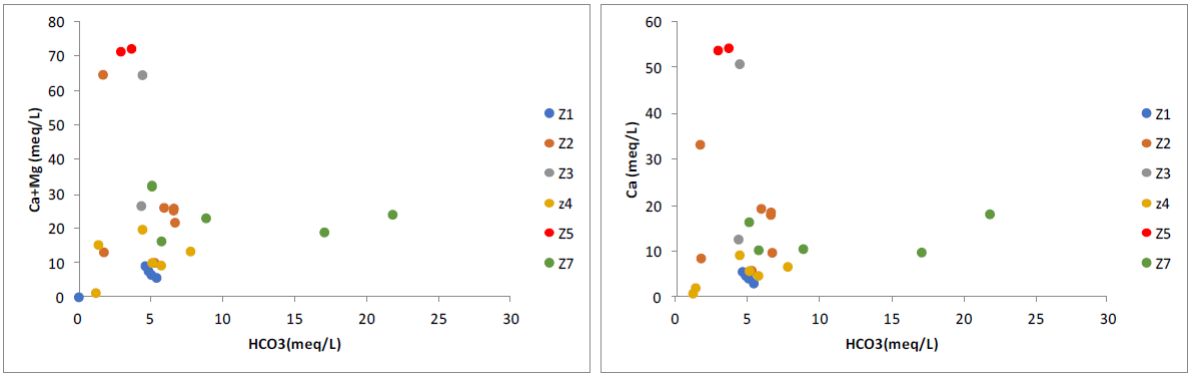


Figure 6. (Left) Correlation between the sum of calcium and magnesium ions and bicarbonate; (Right) Correlation between calcium and bicarbonate ions in the analyzed samples.

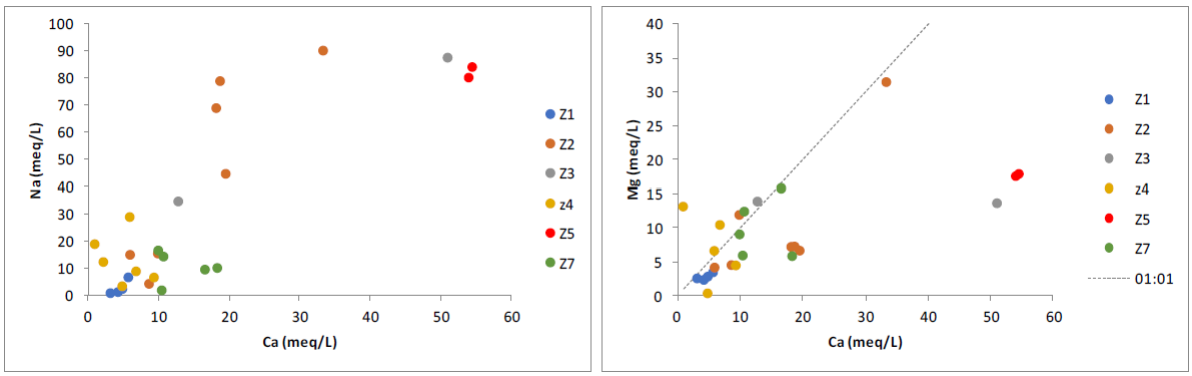


Figure 7. (Left) Plot of sodium (Na+) concentrations against calcium (Ca2+) concentrations; (Right) Plot of magnesium (Mg^{2+}) against calcium (Ca^{+}) concentrations, including the 1:1 correlation line (meq/L).

3.1.2 Chemical Composition of the Gas Phase

Assigning a precise origin to gaseous components is complex due to isotopic disequilibrium processes (such as 18O exchange with host rocks) and fractionation during dissolution/exsolution phases. However, the analysis of the free gas phase detected in the Gourougou/Driouch and Pre-Rif to Meso-Rif zones reveals distinct geochemical signatures (Table 1).

- Gourougou/Driouch Zone (Samples Z2.4, Z2.5): The gas phase is dominated by Nitrogen (N2), ranging from 78.1% to 91.5%, with moderate CO2 levels (2.7% to 12.9%). A critical finding is the high concentration of Helium (He), reaching up to 923 ppm (Z2.4), associated with Neon (Ne) concentrations between 10 and 12 ppm.

- Pre-Rif to Meso-Rif Zone (Sample Z7.2): In contrast, this zone is characterized by a CO2 dominant phase (78.3%), with subordinate N2 (17%) and significantly lower Helium concentrations (10 ppm). The high CO2 content suggests saturation of the fluids at depth and rapid ascent along permeable structures, reaching the surface relatively unchanged.

Table 1: Composition of the gaseous phase associated with the studied thermal waters, determined by gas chromatography; nd denotes not detected.

Sample	O_2 %vol	N_2 % vol	CH_4 ppm	CO ppm	CO_2 % vol	H_2 % vol	He ppm	Ne Ppm	Ar Ppm
Free Gas Phase									
Z2.4	6.6	78.1	278	n.d.	12.9	n.d.	923	10.33	7534.02
Z2.5	0.7	91.5	24800	n.d.	2.7	n.d.	151	12.31	8298.24
Z7.2	2.9	17.1	70	5	78.7	n.d.	10	2.46	3403.23
Dissolved Gas Phase (CcSTP/L)									
Z2.1	1.09	17.36	3.3E-04	3.3E-04	58.4	2.7E-04	2.4E-03	—	—
Z2.4	0.83	15.77	9.7E-03	n.d.	132.9	2.4E-04	1.0E-02	—	—
Z2.5	0.06	20.67	8.1E-02	n.d.	17.8	n.d.	3.0E-04	—	—
Z3.2	0.65	12.35	6.0E-03	n.d.	48.7	n.d.	n.d.	—	—
Z5.2	3.74	11.52	4.6E-05	5.6E-05	16.3	n.d.	9.0E-05	—	—
Z7.2	3.65	8.21	1.7E-03	n.d.	413.6	n.d.	n.d.	—	—

Noble gases serve as tracers for deep crustal migration (ex. Snyder et al. 2001, 2003). The projection of gas samples on the N2-Ar-He ternary diagram (see Figure 5) highlights two distinct origins:

- The Gourougou samples plot above the Air Saturated Water (ASW) line with N2/Ar ratios between 104 and 110, indicating a significant magmatic or deep crustal contribution.
- The Pre-Rif sample plots within the atmospheric field (N2/Ar ≈50), suggesting a predominantly meteoric origin with limited deep inputs, despite the high CO2.

Hydrogen (H2) was not detected, likely due to re-equilibration or loss during ascent. Dissolved gas compositions (Table 3) further reflect solubility-controlled fractionation processes distinctive from the free gas phase.

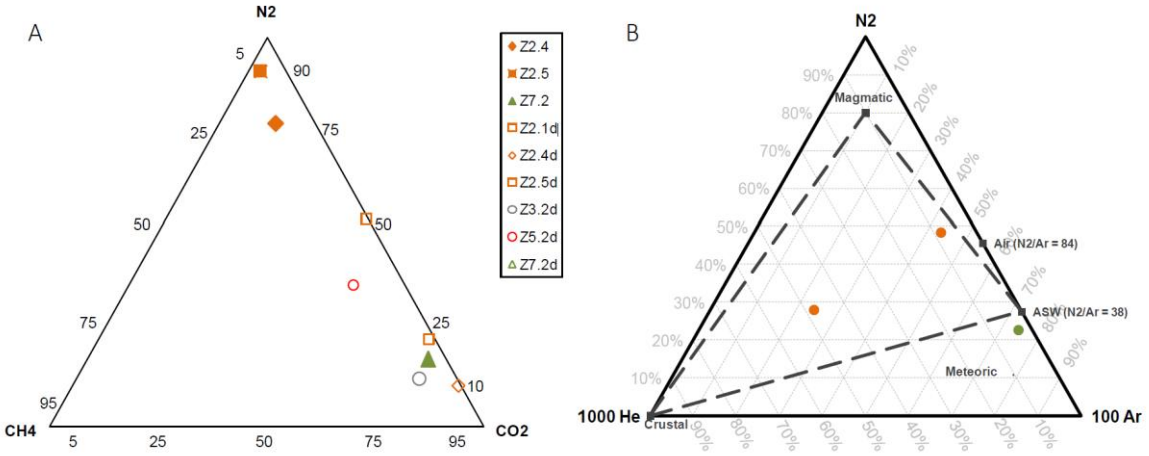


Figure 7. (Left) CO_2-CH_4-N_2 Ternary Diagram showing the projection of the sampled free and dissolved (d) gas compositions; (Right) Ar-N_2-He Ternary Diagram showing the projection of free gas samples (Zone 2 in orange, Zone 7 in green).

3.1.3 Isotopic Composition of Liquid and Gaseous Phases

The stable isotope analysis indicates a meteoric origin for the geothermal fluids. As shown in (Figure 7) (Diagram δ2H vs δ 18O), the samples cluster near the Global Meteoric Water Line (GMWL) and the Local Meteoric Water Line (LMWL), confirming that the water originates from precipitation. A slight deviation indicating evaporation effects, consistent with the semi-arid climate, is observed, aligning with previous regional studies (Winckel et al., 2002).

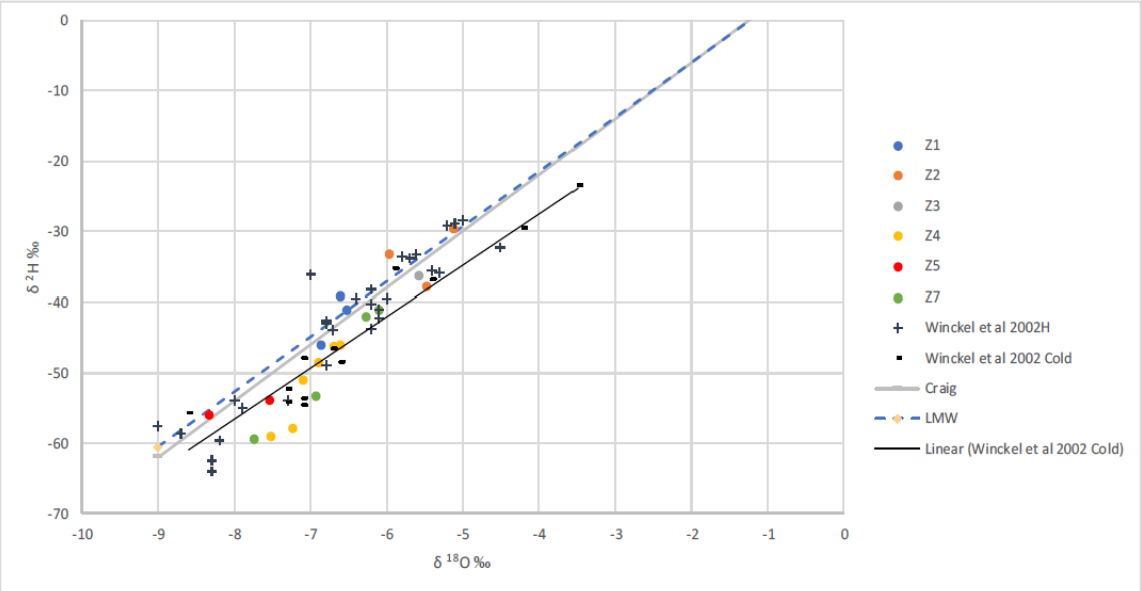


Figure 8. Plot of isotopic ratios (δ^2H vs $\delta^{18}O$) for the sampled waters, showing the Global Meteoric Water Line (GMWL, or Craig) and the Local Meteoric Water Line (LMW) according to (Cidu & Bahaj, 2000)**. The figure also displays the isotopic composition of mineral waters (+) and cold shallow borehole waters (-) from** (Winckel et al., 2002)**, along with the line defined by the shallow borehole compositions.**

The isotopic signature also serves as a tracer for recharge elevation, revealing distinct catchment areas:

- Gourougou/Driouch & Arekman Zones: Enriched isotopic values indicate recharge at low altitudes (< 250 m) or proximity to the coast.
- Ain Goutitir/Taourirt Zone: Depleted values point to a recharge zone at higher elevations, estimated between 700 and 750 m.
- Pre-Rif to Meso-Rif Zone: This area exhibits the lightest isotopic composition, suggesting recharge at high altitudes exceeding 1000 m.

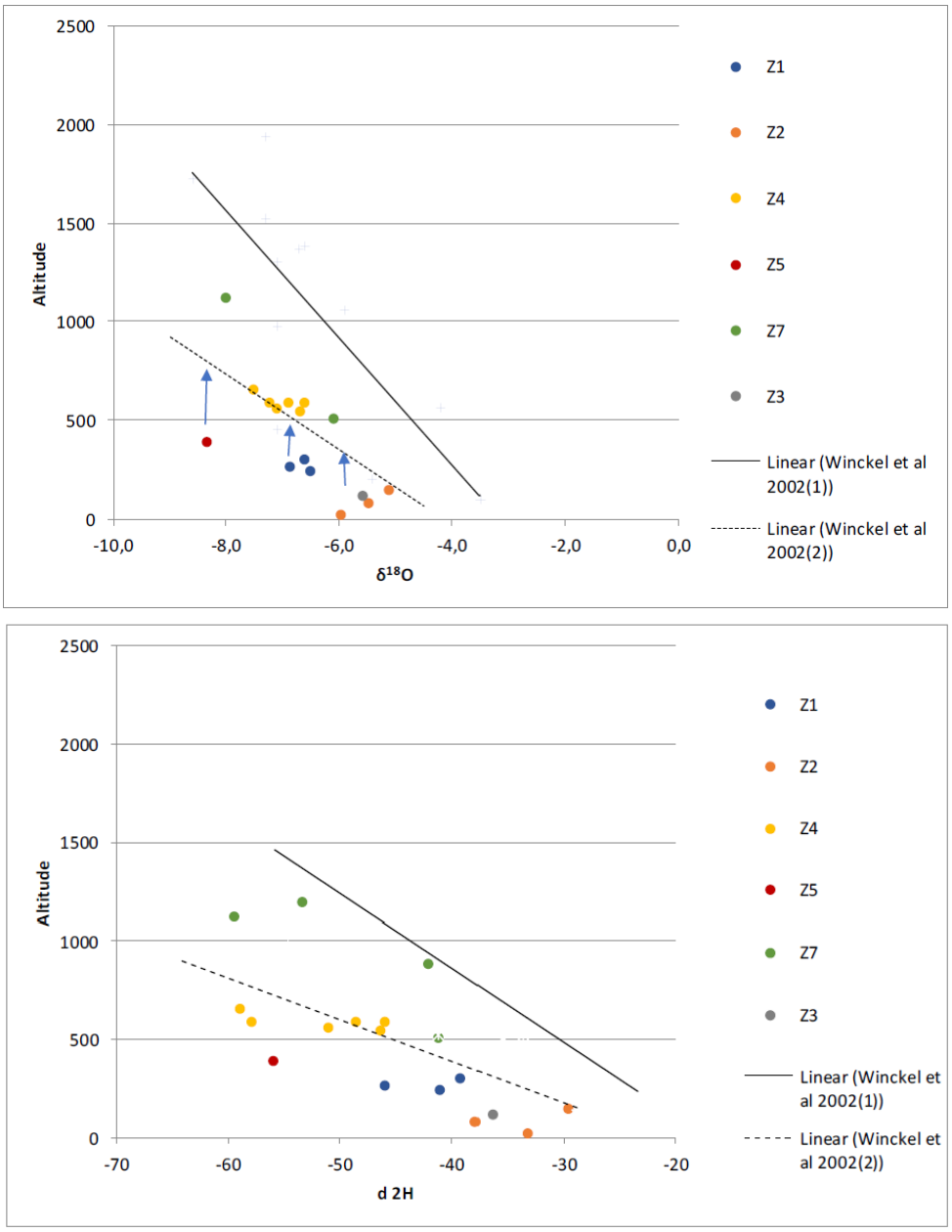


Figure 9. (Top) Relationship between the isotopic composition (δ^2H vs $\delta\ ^{18}O$) of sampled water and recharge altitude, showing the projection of thermal (2) and cold (1) data (Winckel et al., 2002) and derived correlation lines; (Bottom) Relationship between the isotopic composition ($\delta\ ^2H$) of sampled water and source altitude, showing the correlation lines defined by the projected thermal (2) and cold (1) data (Winckel et al., 2002).

Isotopic ratios of Carbon (13C), Helium (3He/4He), and Radon (222Rn) concentrations were analyzed to constrain the depth and origin of the fluids.

- Carbon Isotopes: The δ 13C values in dissolved CO2 suggest a mixed origin. However, sample Z7.2 exhibits a primitive carbon signature, potentially indicating deep crustal or mantle degassing. Conversely, isotopic analysis of methane (CH4) in sample Z2.5 reveals a fractionation factor (αc = 1.041) consistent with a biogenic origin (fermentation) rather than thermogenic processes.

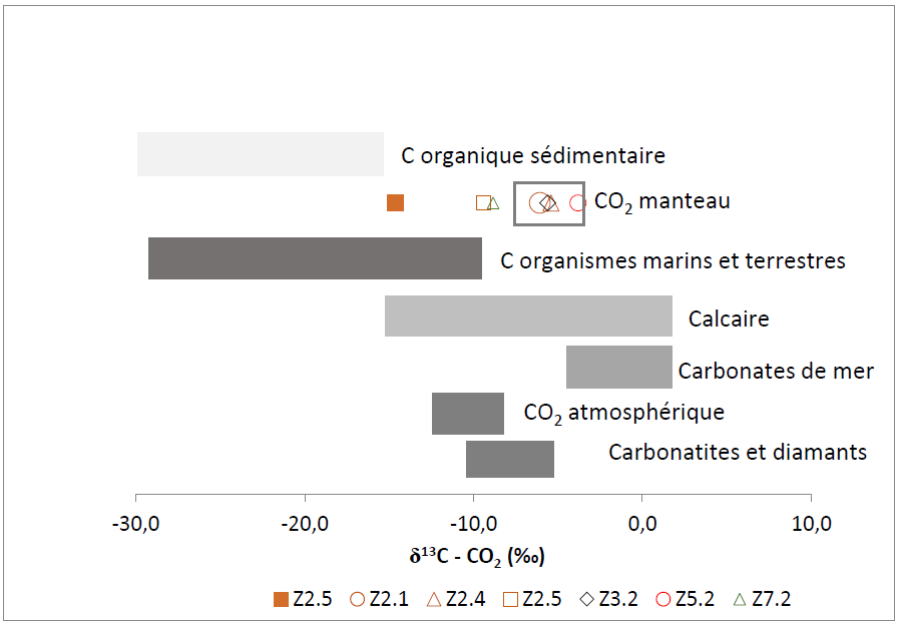


Figure 10. δ ^{13}C isotopic composition of CO_2 in sampled thermal fluids (free and dissolved phases), compared to common δ ^{13}C values from various organic, crustal, and mantle environments.

- Noble Gases (Helium): The 3He/4He ratios (R/Ra) provide critical evidence for the heat source. In the Gourougou/Driouch volcanic zone, ratios range from 0.13 to 0.73 Ra, which are significantly higher than typical crustal production values (~0.02 Ra). This confirms a distinct magmatic/mantle component in the fluids, supporting the presence of deep-seated intrusions.

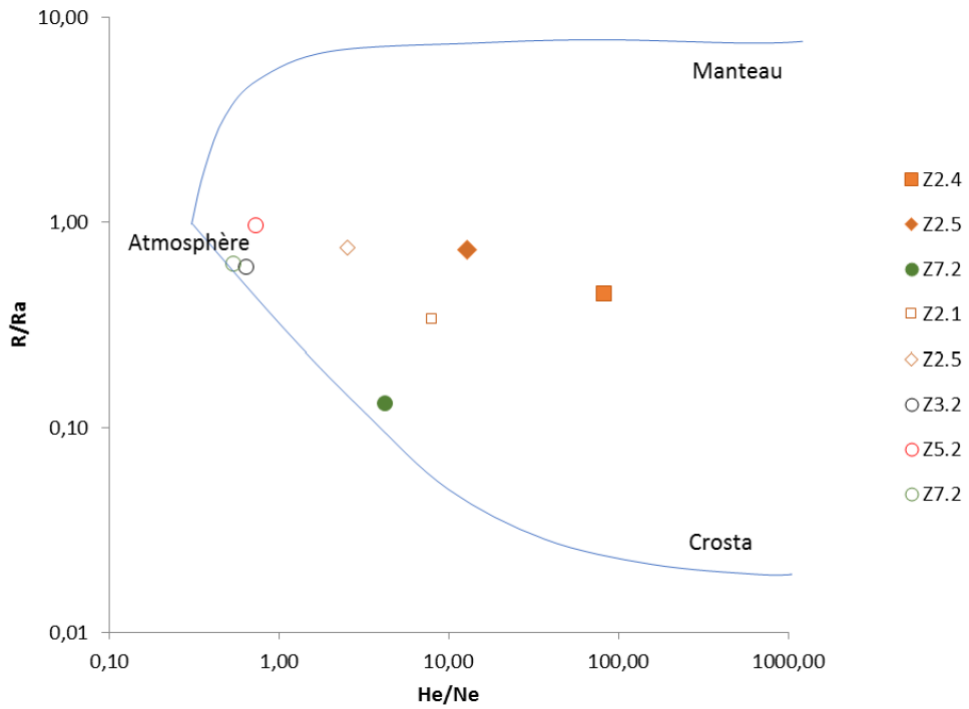


Figure 11. Projection of the isotopic ratios R/Ra vs He/Ne for the free (solid symbol) and dissolved gas phases.

- Radon (222Rn): While most samples show low radon content, the Gourougou/Driouch zone (sample Z2.4) presents an anomalously high concentration of 565.2 Bq/L. This high radioactivity, associated with the free gas phase, confirms the existence of a highly permeable fracture network facilitating the rapid ascent of deep gases to the surface.

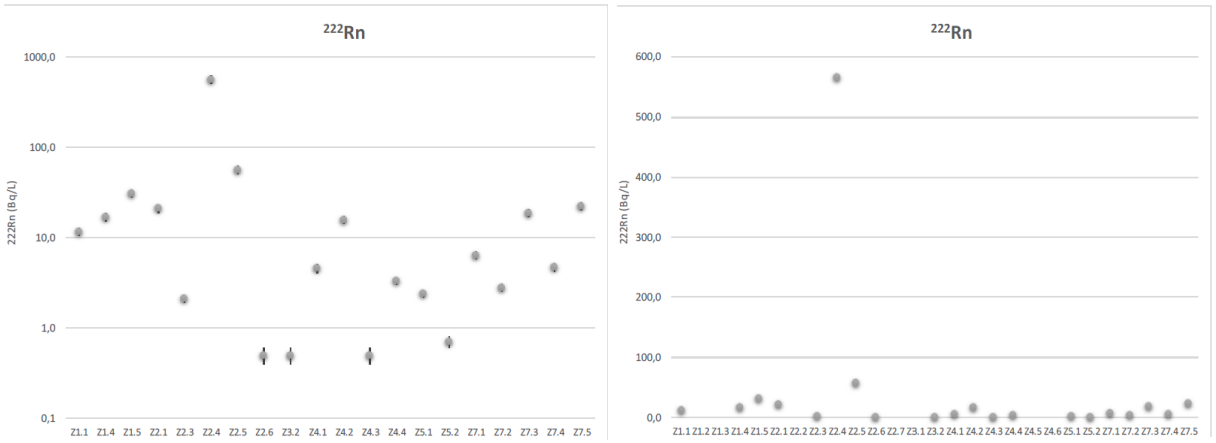


Figure 12. Comparison of Radon-222 (^{222}Rn) concentration in sampled waters: logarithmic scale representation (left) versus decimal scale representation (right)

3.2 Thermodynamic Modeling and Saturation Indices

To assess the thermodynamic state of the geothermal fluids and predict potential scaling or dissolution processes, Saturation Indices (SI) were calculated for relevant mineral phases. The SI is defined as $SI = log(Q/K)$, where Q is the ion activity product and K is the equilibrium constant at a given temperature.

The activity of mineral phases containing less than 5–10% solid solution was assumed to be unity, following the approximation by (Helgeson et al., 1970). To interpret the fluid-mineral equilibrium, a specific tolerance range was applied to account for analytical and thermodynamic uncertainties. In accordance with (Nordstrom & Jenne, 1977) and (Lee & Strickland, 1988), the equilibrium state is defined within the range of -0.1 ≤SI≤+0.1. Values of SI > +0.1 indicate supersaturation (potential precipitation), while values of SI < -0.1 indicate undersaturation (potential dissolution).

All thermodynamic calculations and speciation modeling were performed using the PHREEQC geochemical code, utilizing the standard phreeqc.dat thermodynamic database.

The thermodynamic behavior of the fluids was analyzed by calculating Saturation Indices (SI) for key mineral phases (Carbonates, Silica, Evaporites, and Aluminosilicates). The results, illustrated in (Figures 13 to 15), reveal distinct geochemical environments.

3.2.1 Carbonate Equilibrium (Reservoir Signature)

The majority of thermal waters, particularly in the Berkane/Fezouane and Oujda/Angads zones, are in equilibrium or slight supersaturation with respect to Calcite, Aragonite, and Dolomite.



Figure 13 . Plot of the saturation index (log SI) of waters in the Berkane/Fezouane zone with respect to various mineral phases

This equilibrium confirms that the fluids circulate within and chemically equilibrate with the Liassic carbonate reservoir (limestones and dolomites).

Except in the Gourougou/Driouch zone, while most waters are supersaturated, sample Z2.1 shows undersaturation, likely due to mixing with shallower, colder waters.

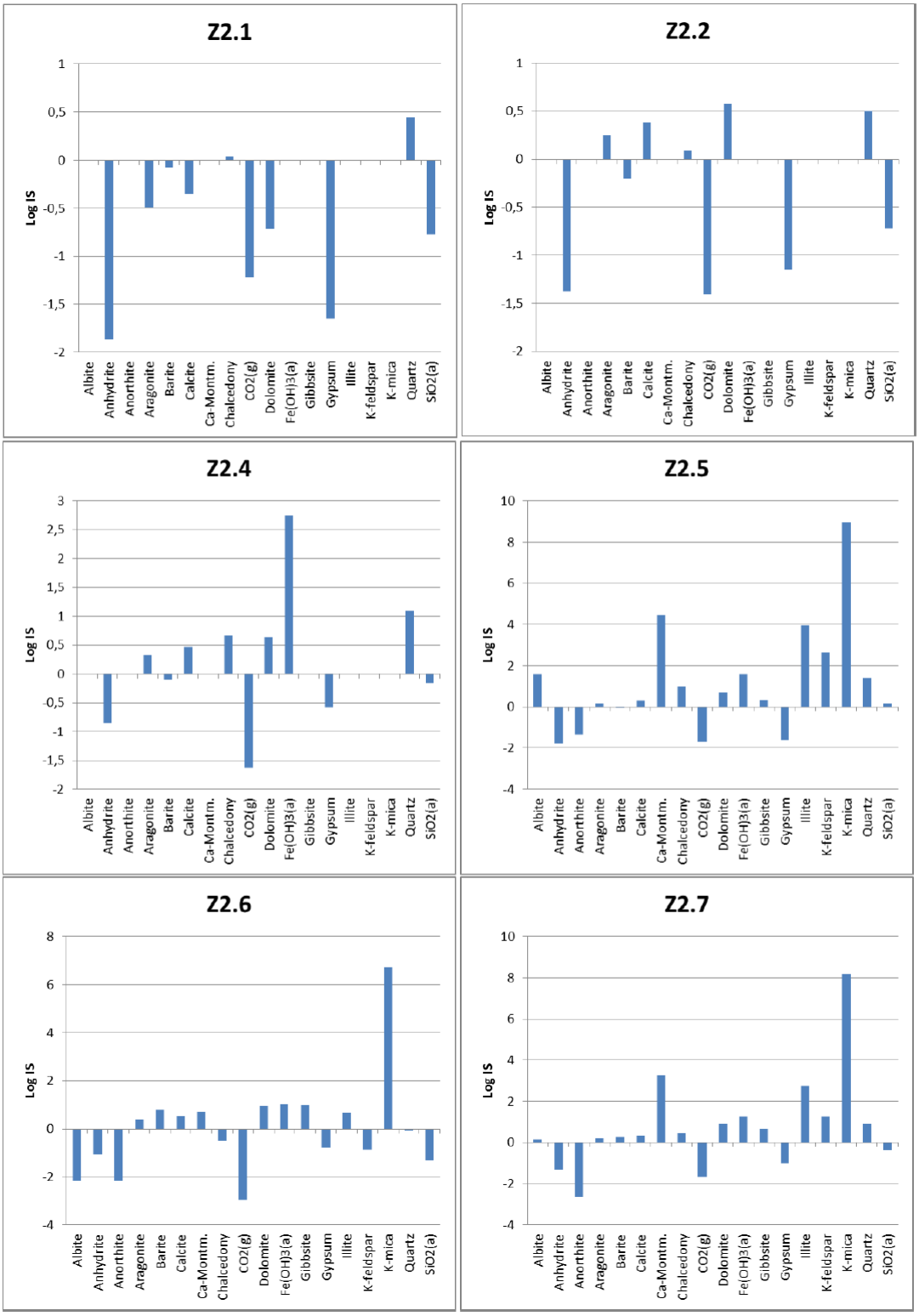


Figure 14. Plot of the saturation index (log SI) of Kert River water (Gourougou/Driouch zone) with respect to several solid and gaseous mineral phases.

3.2.2 Silica Phases (Thermal History)

A generalized supersaturation with respect to Quartz is observed across most zones, while Chalcedony is frequently near equilibrium (e.g., in Berkane and Pre-Rif zones).

This pattern indicates that the fluids equilibrated at higher temperatures at depth (controlling Quartz solubility) and cooled during ascent, leading to supersaturation at surface conditions. This validates the use of silica geothermometers for these systems.

3.2.3 Evaporites and Salinity Source

Despite the high salinity observed in the northern zones, all samples remain undersaturated with respect to Halite.

The Ain Goutitir/Taourirt zone (Sample Z5.2) is the only one showing thermodynamic equilibrium with Gypsum. This provides geochemical proof that these fluids circulate through gypsiferous formations (likely Triassic evaporites), explaining their high mineralization and distinct chemical facies compared to the carbonate-hosted waters of Berkane.

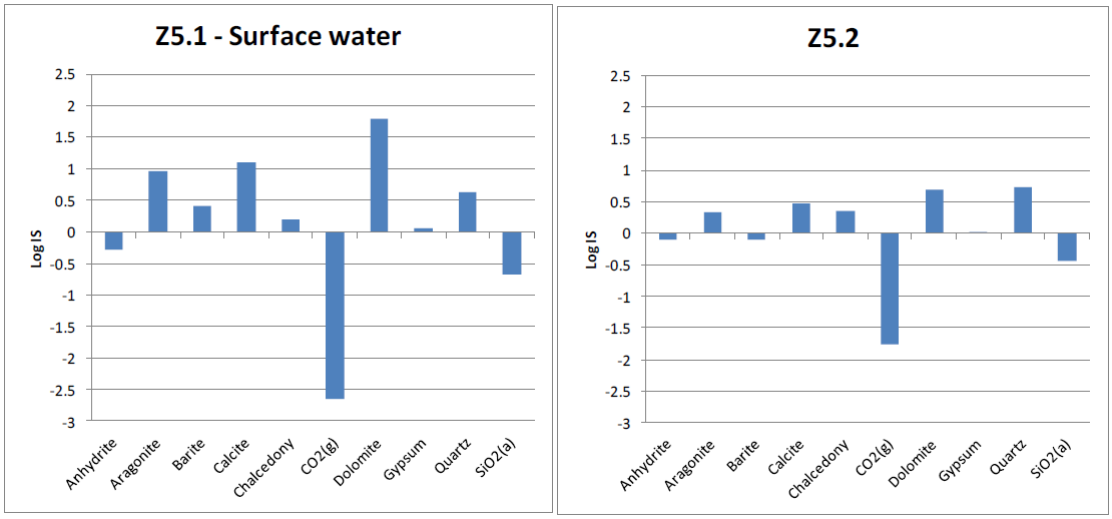


Figure 15. . Plot of the saturation index (log SI) of Kert River water (Ain Goutitir/Taourirt) with respect to several solid and gaseous mineral phases

3.2.4 Redox Indicators and Aluminosilicates

- Iron Hydroxides: In the Gourougou/Driouch and Arekman zones, waters are supersaturated with iron hydroxides. This suggests a rapid transition from deep, reducing conditions to an oxidizing surface environment, leading to the precipitation of amorphous iron oxides.

- Aluminosilicates: Most waters are undersaturated with respect to primary aluminosilicates but show saturation with secondary clay minerals (K-mica, Ca-montmorillonite), reflecting active hydrolysis and alteration of the host rocks (schists or volcanic tuffs).

- Gas Pressure: High partial pressures of CO2 (PCO2) are inferred from the saturation indices in the Gourougou zone, consistent with the presence of free gas phases

3.3 Geothermometry Approach

Estimating reservoir temperatures is complex due to cooling during fluid ascent and mixing with shallow cold aquifers. To address these uncertainties, a combined approach using qualitative indicators, quantitative chemical geothermometers, and multi-mineral equilibrium modeling was applied. It is important to note that while standard geothermometers are calibrated for high-enthalpy volcanic systems, their application in the sedimentary, medium-enthalpy context of Northeastern Morocco requires careful interpretation (Fournier & Potter, 1979; Fournier & Truesdell, 1973).

3.3.1 Qualitative and Quantitative Indicators

Preliminary assessment relied on qualitative indicators: high concentrations of dissolved gases (CO2, H2) or volatile elements (B, F, Hg, As) suggesting high temperatures, and the presence of travertine deposits indicating potential cooling or mixing.

Quantitative estimation employed standard empirical equations:

- Silica Geothermometers: Based on the temperature-dependent solubility of silica species (Quartz, Chalcedony, Amorphous Silica). Equations by (Fournier & Truesdell, 1973) were applied. These are generally reliable but can be affected by dilution or evaporation.

- Cation Geothermometers: Based on temperature-dependent ion exchange reactions (e.g., feldspars/clays). We utilized Na/K (Giggenbach, 1988), Na-K-Ca (Fournier & Truesdell, 1973), and K/Mg(Giggenbach, 1988) geothermometers.

In Northeastern Morocco, high salinity (marine origin) and high Magnesium content can lead to overestimated temperatures using Na-K-Ca. Therefore, the K2/Mg geothermometer was prioritized for lower temperature or immature waters, as suggested by Giggenbach (1988).

3.3.2 Multi-mineral Equilibrium and Isotopic Geothermometry

To overcome the limitations of individual geothermometers, particularly in mixed waters, the Multi-mineral Equilibrium approach (Reed & Spycher, 1984) was applied using PHREEQC. This method identifies the temperature at which the Saturation Indices (SI) of a specific mineral assemblage converge to zero, representing the likely reservoir equilibrium temperature.

Additionally, for gas-rich samples (e.g., Z2.5), isotopic geothermometry based on carbon fractionation between CO2 and CH4 (δ 13C) was used to constrain deep equilibrium temperatures.

Table2. Temperature and reservoirs depth estimate

Zone	Reservoir temperature by Geothermometer			Reservoir			geothermal gradient (°C/km) (in brackets)
	Silica	Cation	multi-mineral	Formation/ Age	Depth min (m)	Depth max (m)	
Berkane/ Fezouane	<75°C	<70°C	60°C to 75°C	1624/7[(1)], Limestone and dolomite /Lias	896	1228	1631-7[(1)] (45.2)
Gourougou / Driouch	<180-185°C	<200°C	<175°C	Jurassic of the Temsamane massif	653	1829	(85) according to the gradient map of the figure 14
Arekman/ Ras El Ma	<100°C	<100°C	75°C to 100°C	Arekman/Lias	694 1463	1006 - 2073	Nador1[(2)] (41) Arekman[(1)] (80)
Oujda/ Angads	90°C	--	75°C to 125°C	Limestone and dolomite /Lias	1156	1960 - 2664	2952-12[(1)] (48)/
Ain Goutitir/ Taourirt	<106°C	<100°C	80°C to 110°C	Limestone and dolomite /Lias	1729	2586	MSD1[(2)], GRF1[(2)], KDH1[(2)] (35)
Pré-Rif to Méso-Rif	100-125°C	<120°C	>100 to150°C	Limestone and dolomite /Lias	1635	2446	AKL101[(2)], ATM1[(2)] (37)

[(1)] Groundwater well, [(2)] Oil well

3.4 Geothermal Gradient and Heat Flow Determination

To establish a reliable thermal model of the crust, a dual approach was applied, combining direct local measurements in boreholes with a regional geophysical estimation derived from magnetic data.

3.4.1 Direct Temperature Acquisition (Borehole Data)

To generate the regional geothermal gradient and heat flow maps, a geostatistical interpolation was performed using the Kriging method on data derived from mining, hydraulic, and petroleum boreholes (Figure 16, right). To ensure regional consistency and minimize boundary effects, the dataset was harmonized by integrating available thermal data from neighboring regions, specifically the Alboran Sea and Algeria. The thermal data used for this interpolation were acquired and corrected as follows:

- Shallow Boreholes (100–500 m): High-resolution continuous temperature profiles were acquired in boreholes that had reached thermal equilibrium using Antares and MTL loggers. The upper 30–50 m were excluded to avoid seasonal climatic perturbations1.

- Deep Wells (>750 m): Bottom Hole Temperatures (BHT) from oil exploration wells were utilized. Raw BHT data were corrected for drilling disturbances using the Horner plot method or standard correction curves calibrated for North African sedimentary basins (e.g., (Takherist & Lesquer, 1989)).

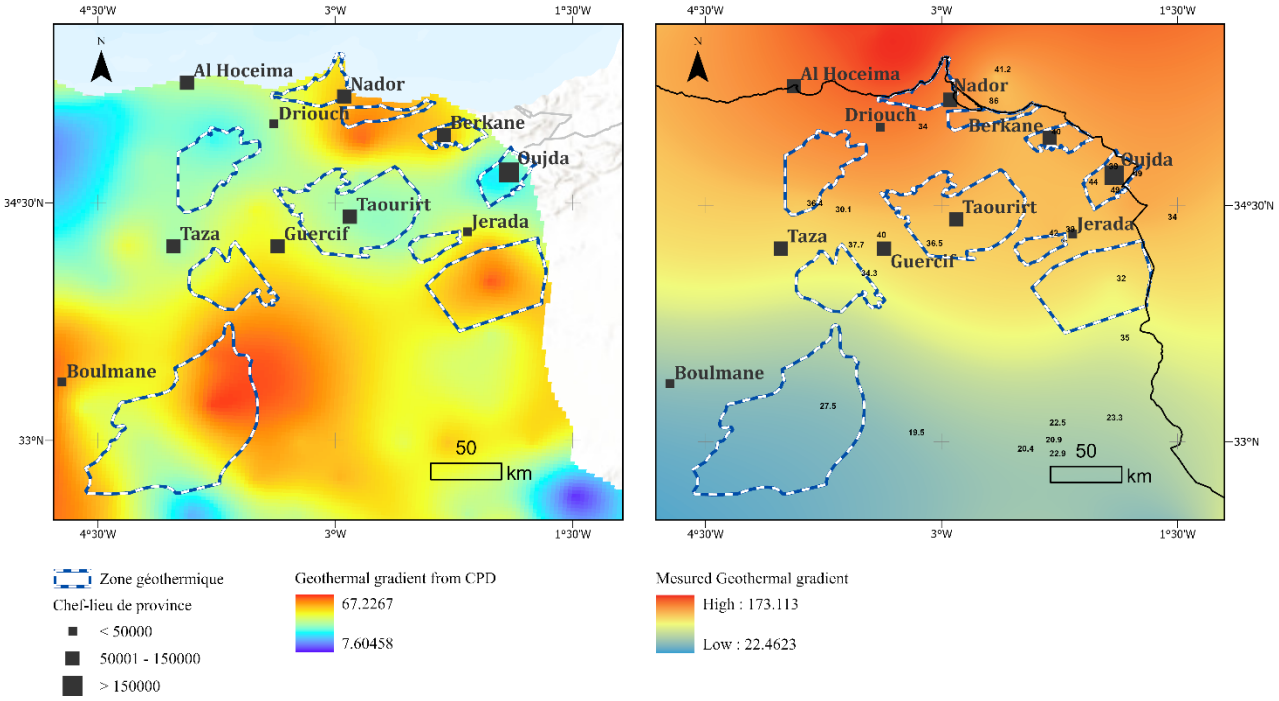


Figure16. Regional geothermal gradient assessment. (Left) Map estimated from spectral analysis of magnetic data (Curie Point Depth); (Right) Map obtained through Kriging interpolation of direct temperature logs, where overlaid numbers indicate the specific geothermal gradient values measured at each well.

3.4.2 Geophysical Estimation via Magnetic Data

To extend the thermal assessment beyond available well data, a regional estimation of the geothermal gradient and heat flow was derived from the spectral analysis of aeromagnetic data, as established by(Boumehdi et al., 2025)

- Curie Point Depth (CPD): The depth to the Curie isotherm (approximately 580 °C for magnetite) was mapped using the power spectrum method (centroid method) applied to magnetic anomaly data.

- Thermal Calculation: The CPD acts as a deep isothermal boundary. By assuming a conductive heat transfer model, the vertical geothermal gradient (dT/dz) was calculated between the surface and the CPD. Subsequently, the heat flow density (q) was derived by combining this gradient with the regional thermal conductivity model ($q = \lambda \, dT/dz$). This method allows for the detection of deep thermal anomalies associated with crustal thinning and magmatic intrusions that might be missed by sparse well data.

3.4.3 Thermal Conductivity and Heat Flow Calculation

- Conductivity (λ): For available rock samples, thermal conductivity was measured in the laboratory using the ISOMET 2104 heat transfer analyzer. For deep sections without cores, in-situ conductivity was estimated using a geometric mixing model based on mineralogical composition (quartz, calcite, clay) and porosity variations5.

- Heat Flow (q): Surface heat flow density from boreholes was calculated using the Bullard Plot method (Thermal Resistance method). Furthermore, the contribution of Radiogenic Heat Production (A) was

assessed by analyzing Uranium (U), Thorium (Th), and Potassium (K) concentrations via gamma-ray spectrometry, allowing for corrections of crustal heat generation.

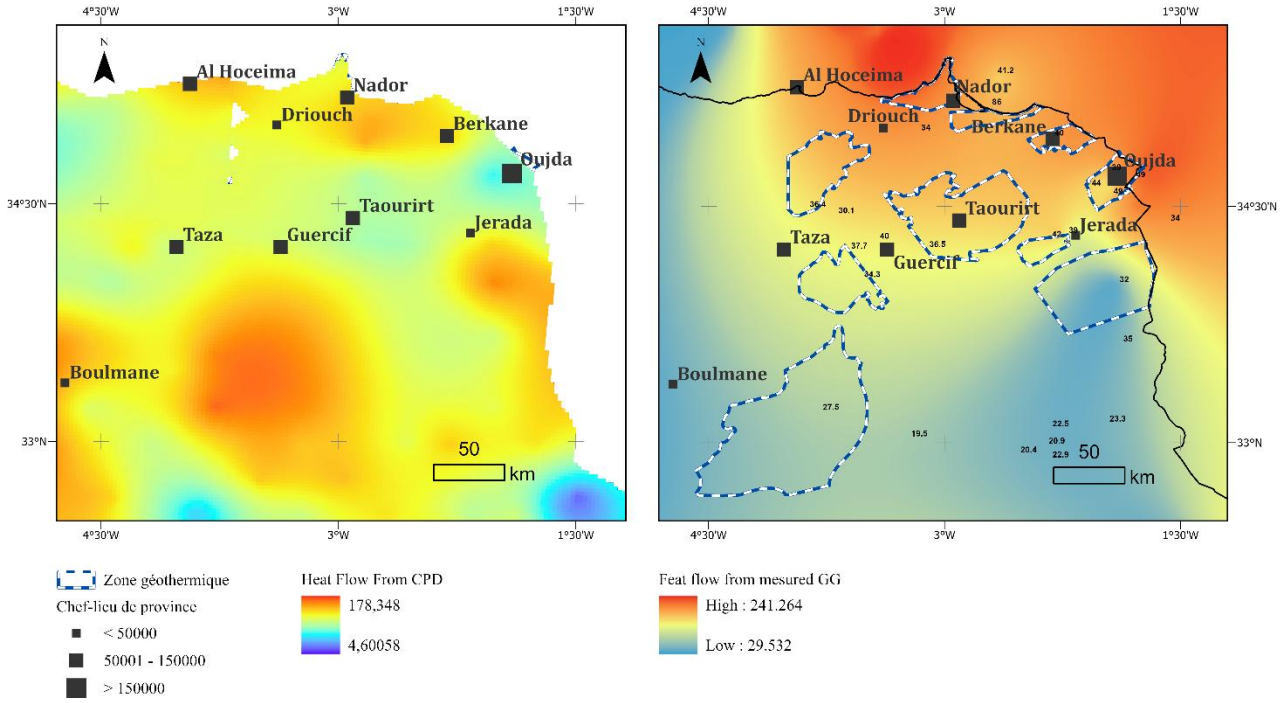


Figure17. Regional heat flow density assessment. (Left) Map estimated from spectral analysis of magnetic data (Curie Point Depth); (Right) Map obtained through Kriging interpolation of calculated heat flow values, where overlaid numbers indicate the specific heat flow densities determined at each well.

3.5 Geophysical Data and Lineament Extraction (GGM+)

To overcome the limitations of unevenly distributed ground gravity data in Northeastern Morocco, this study utilized the Global Gravity Model plus (GGM+). Developed by (Hirt et al., 2013), this composite model integrates satellite gravity information (from GRACE and GOCE missions) with high-resolution topographic data (SRTM) to provide gravity disturbance fields at an ultra-high resolution of approximately 200 m (~0.2 km). This resolution is critical for detecting both regional crustal structures and local fault networks controlling hydrothermal circulation.

Prior to edge detection, a Spectral Analysis was performed to characterize the signal's frequency content. By plotting the logarithm of the radially averaged power spectrum against the wavenumber (Figure 18), we differentiated between low frequency anomalies corresponding to deep crustal discontinuities and high-frequency signals associated with shallow sedimentary structures, allowing for an estimation of the mean depth of the causative sources.

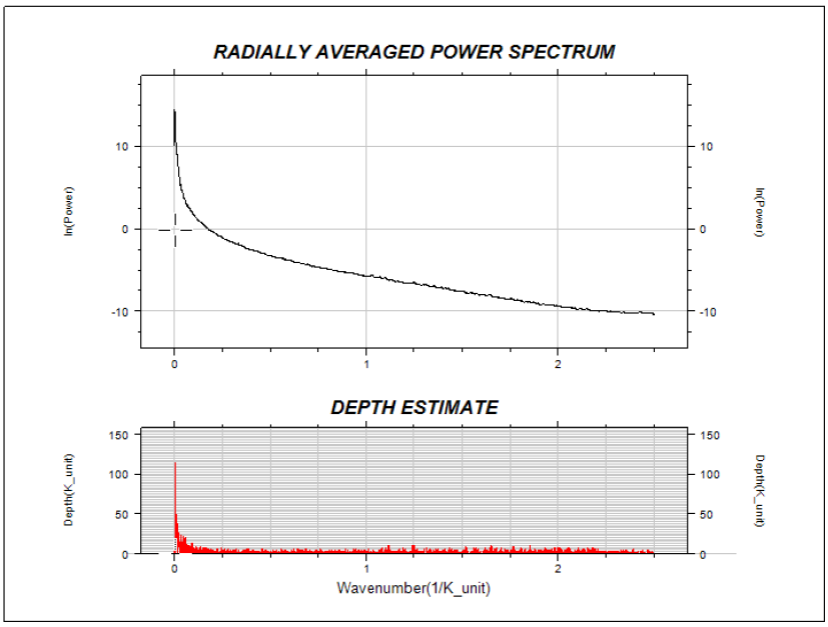


Figure17. Radially averaged power spectrum of GGM+ gravity data..

Lineament Extraction (Multi-Scale Edge Detection): Structural lineaments were delineated using the Multi-Scale Edge Detection method, also known as "worming," following the workflow described by El Gharbaoui et al.. This technique is based on the analysis of the Horizontal Gradient Magnitude (HGM) of the Bouguer anomaly, where the maxima of the gradient correspond to the vertical projection of density contrasts (e.g., faults, geologic contacts).

To determine the vertical continuity and rooting depth of these structures, the HGM maxima were tracked across successive levels of Upward Continuation (ranging from the surface up to deep crustal levels). By stacking these maxima, we generated a "worm map" that differentiates between:

- Shallow lineaments: Visible only at low continuation heights, representing local sedimentary structures.
- Deep-seated faults: Persistent at higher continuation levels, representing major crustal boundaries that act as primary conduits for heat and fluid ascent from the mantle or deep crust.

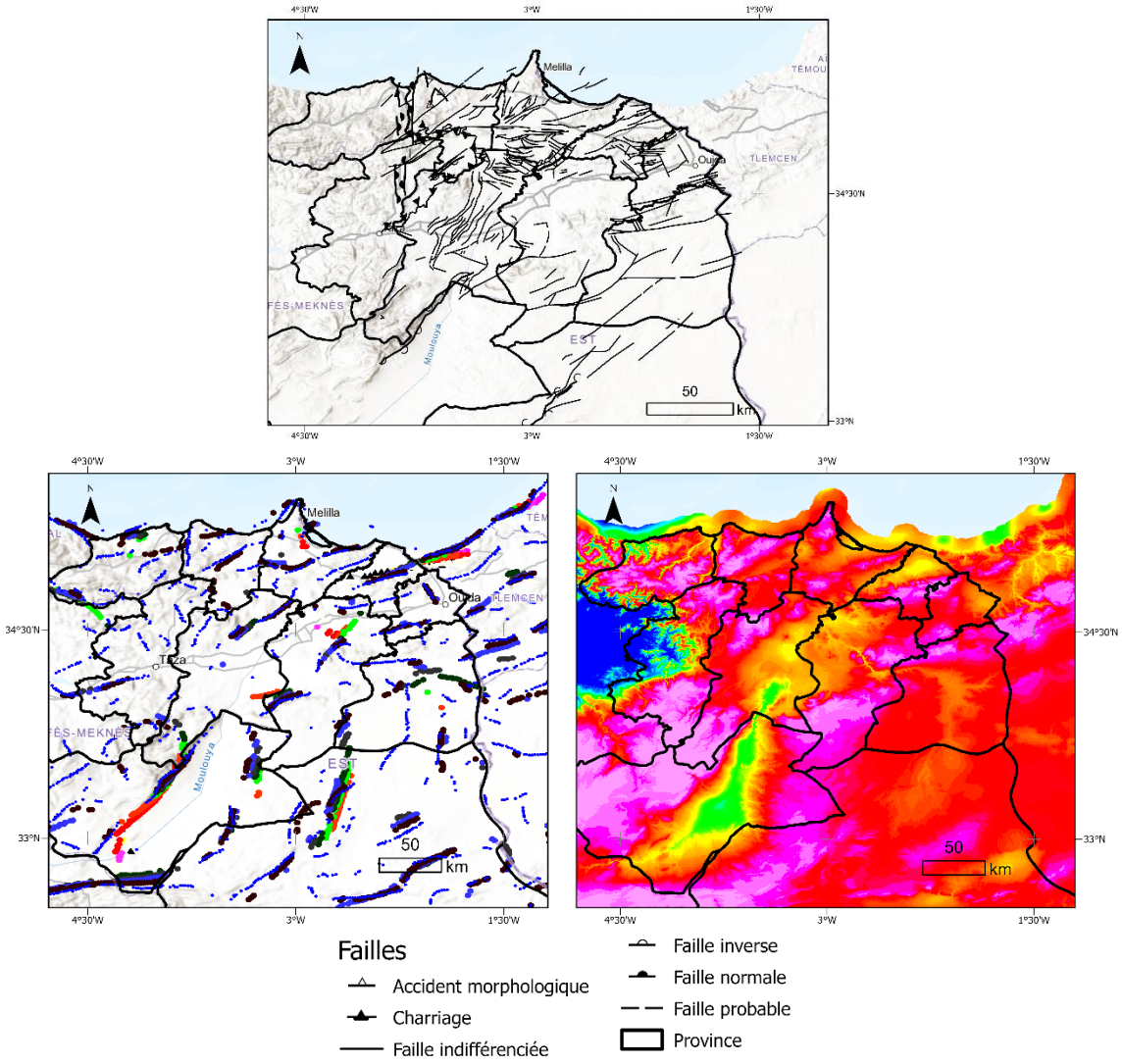


Figure18. Structural and gravimetric analysis of the study area. (Top) Fault network derived from geological mapping; (Bottom Left) Deep lineaments extracted using multi-scale edge detection (worms) from GGM+ data; (Bottom Right) Bouguer anomaly map derived from GGM+ data.

4. RESULTS

4.1. Conceptual Models of Priority Zones

The development of specific conceptual models for the five priority geothermal zones relies on a comprehensive multi-disciplinary synthesis. Beyond the geological structures, borehole temperature profiles, and hydrogeochemical signatures previously detailed, this study integrates critical deep geophysical constraints. High-resolution satellite gravity data (GGM+) were utilized to delineate the deep fracture networks and basement architecture controlling fluid pathways. Furthermore, the regional thermal boundary conditions were refined using geothermal gradients and heat flow density estimates derived from the spectral analysis of aeromagnetic data (Curie Point Depth). This holistic integration allows for a precise definition of the reservoir geometry, heat transfer mechanisms, and fluid dynamics unique to each sector.

4.1.1 Berkane/Fezouane Zone (Triffa Basin)

This zone corresponds to a deep sedimentary basin model situated at the northern flank of the Beni Snassen Mountains.

- Reservoir: The primary reservoir consists of Liassic dolomitic limestones1. These formations outcrop in the Beni Snassen range (recharge area) and plunge northward beneath the Triffa plain, reaching depths exceeding 2000 m in the central Fezouane block.

- Structure: The reservoir is compartmentalized by major NW-SE faults (F1, F2, F3) which act as hydraulic barriers or conduits. Crucially, the gravimetric analysis (GGM+) revealed a deep-seated NE-SW fault intersecting this system. This major deep structure likely acts as the primary regional drain facilitating the ascent of deep geothermal fluids into the compartmentalized reservoir.

- Heat Transfer: Heat transfer is primarily conductive, driven by a high geothermal gradient of 45–50 °C/km. However, local advective anomalies are observed, notably in borehole 1624/7, where the gradient spikes to 127 °C/km at the contact between the impermeable Miocene clays and the carbonate reservoir, indicating upward fluid migration along fault zones.

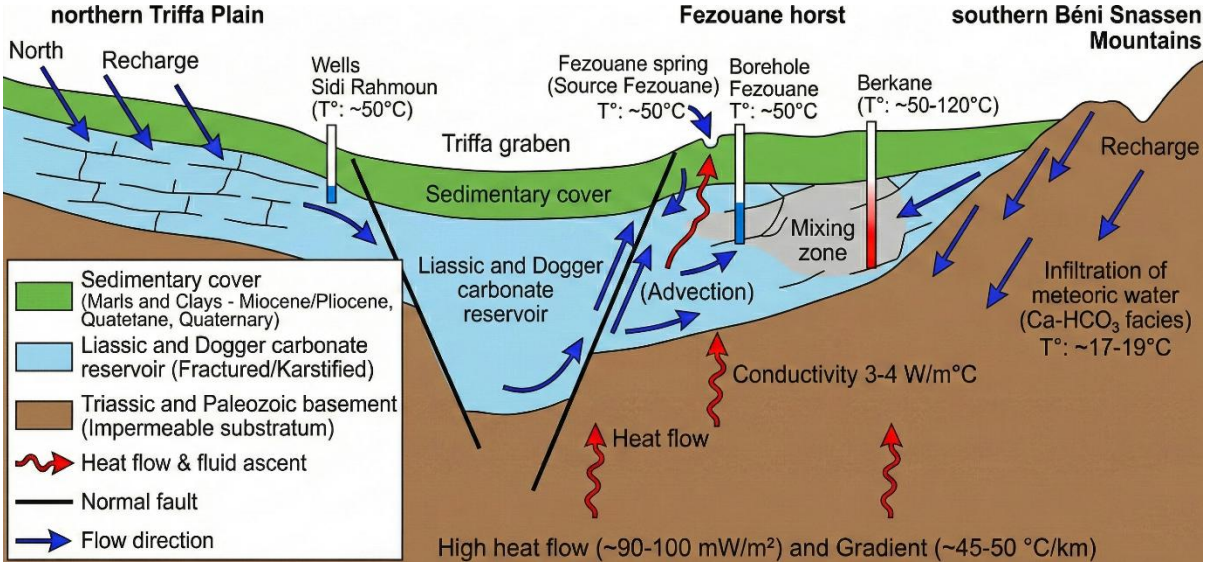


Figure18. Conceptual model of Berkan/ Fezouane zone

4.1.2 Gourougou/Driouch Zone (Eastern Rif)

This zone represents a magmatic-convective system controlled by the Neogene volcanic complex of Gourougou and the intra-rifaine Temsamane unit. Structurally, it is characterized by the most significant crustal thinning in Morocco, with a Moho depth estimated between 20 and 22 km.

- Reservoir: The system is fractured, with fluids circulating within metamorphic schists and overlying volcanic tuffs/rhyolites.

- Heat Source: A strong heat flow density of 120–125 mW/m^2 is directly attributed to this extreme crustal thinning and the presence of shallow magmatic intrusions.

- Fluid Dynamics: Circulation is dominated by convection along deep NE-SW and E-W fractures. The presence of free-phase magmatic gases (CO2, N2) and high Radon content confirms rapid fluid ascent from depth. Recharge occurs at low altitudes, potentially involving seawater mixing, as indicated by the Na-Cl hydrochemical facies.

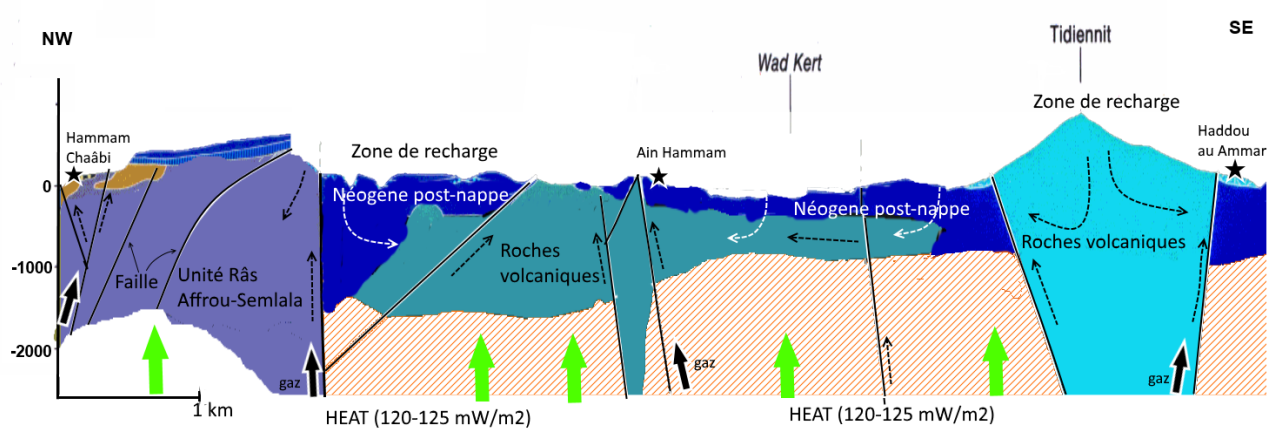


Figure 19. Conceptual model of Gourougou/Driouch zone

4.1.3 Arekman/Ras El Ma Zone (Coastal Rif)

Located east of Nador, this zone shares similarities with the Gourougou system but is heavily influenced by the subsiding Gareb basin structure.

- Reservoir: Exploration well SKA-1 (Kariat Arekman) identified a deep reservoir within fractured rhyolitic and andesitic volcanics at 452 m depth, producing artesian hot water (42°C).
- Structure: The area is structured by horsts and grabens bounded by active faults. Magnetic anomalies suggest the presence of a buried volcanic complex approximately 5 km thick.
- Heat Transfer: The geothermal gradient is exceptionally high, reaching 80 °C/km14. Heat transfer is convective, facilitated by the high permeability of the fractured volcanic rocks and extensional faults.

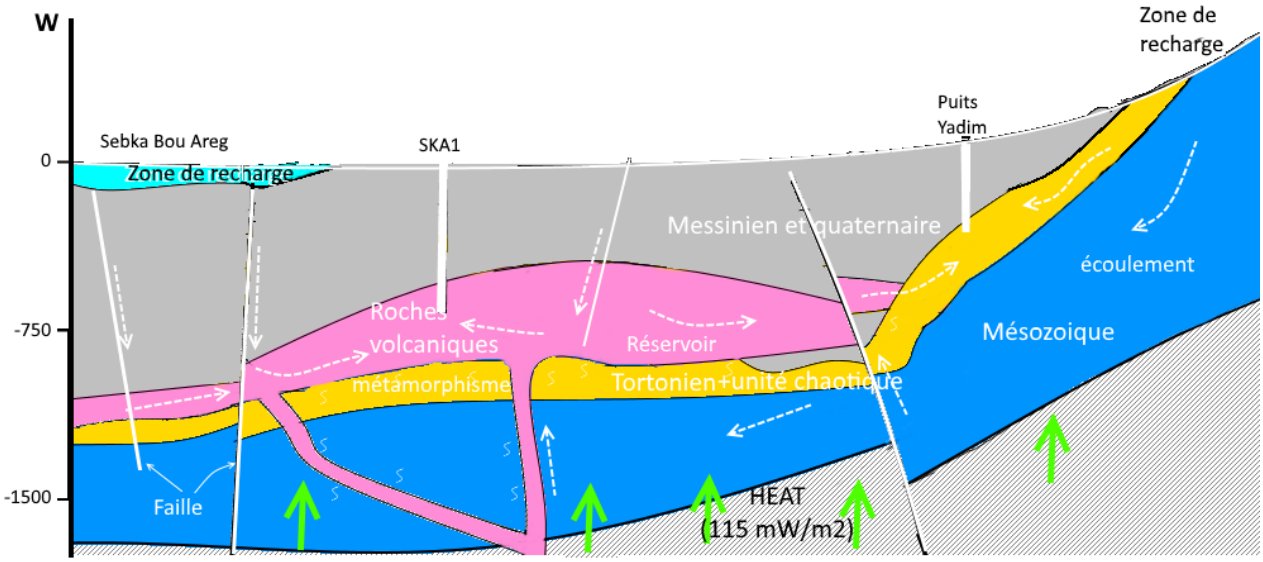


Figure 20. Conceptual model of Arekman/Ras El Ma zone

4.1.4 Oujda/Angads Zone (Horst Chain)

This zone functions as a classic sedimentary basin aquifer system located between the Beni Snassen (North) and the Horst Chain (South).

- Reservoir: The Liassic carbonate platform (Jbel Hamra aquifer) forms a continuous confined reservoir.
- Circulation: Recharge occurs at the southern outcrops (Jbel Hamra). Fluids flow northward, deepening under the thick Miocene marl cover of the Angads plain.
- Discharge: Thermal waters rise along structural highs or faults, as seen at the Ben Kachour artesian borehole (T=54° C), where the reservoir is uplifted. The heat transfer is conductive with a regional gradient of 48–49 °C/km.

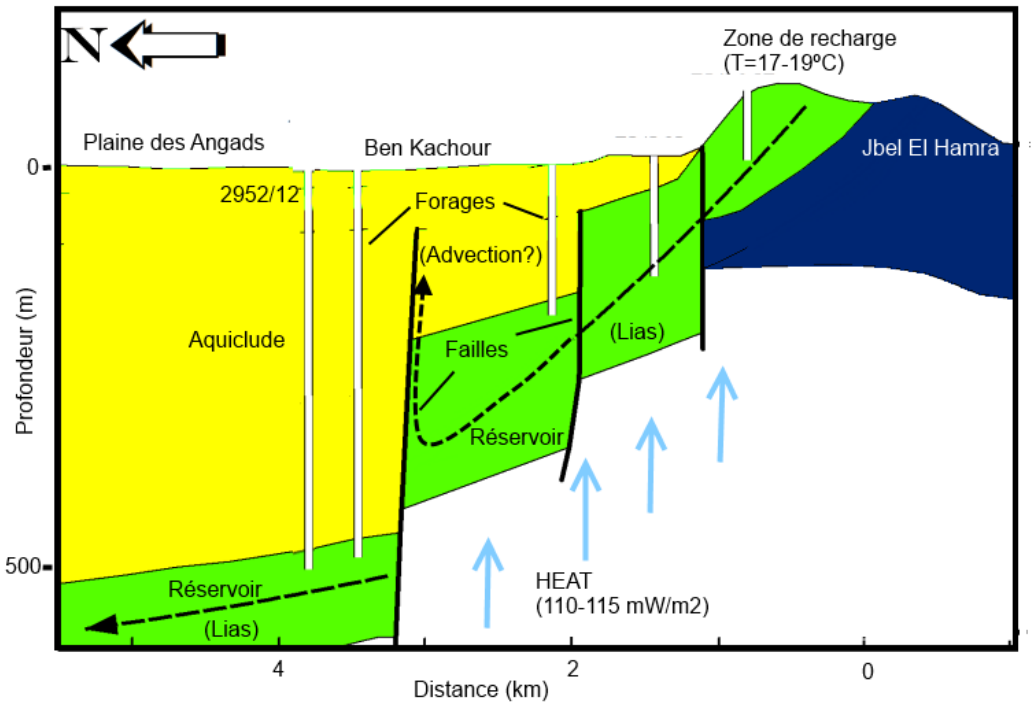


Figure 21. Conceptual model of Oujda/Angads zone

4.1.5 Ain Goutitir/Taourirt Zone (Guercif Basin Margin)

Situated in the Taourirt-Naima corridor, this zone is characterized by significant evaporitic interactions.

- Reservoir: The reservoir comprises Liassic to Dogger dolomitic limestones.
- Geochemistry: Unlike other zones, fluids here show thermodynamic equilibrium with Gypsum, indicating circulation through Triassic or Neogene evaporitic sequences.
- Heat Transfer: The system is conductive-advective, with a gradient of ~45 °C/km. The thermal spring at Sidi Chafi (45° C) and borehole 1212/11 result from rapid ascent along the bounding faults of the Taourirt graben

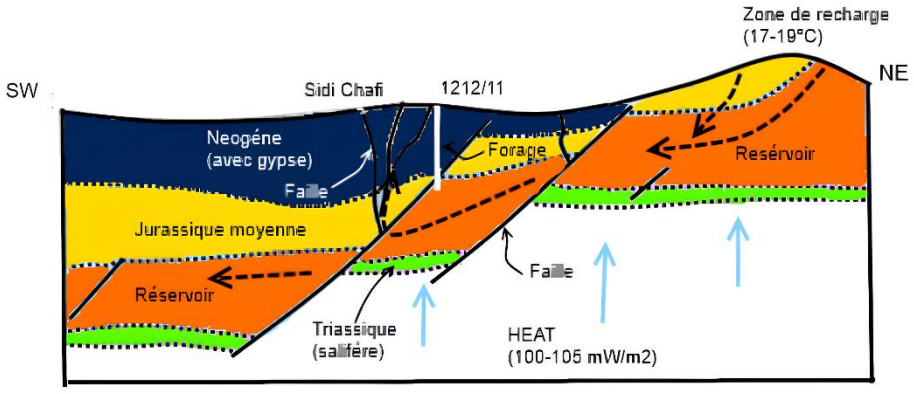


Figure 22. Conceptual model of Oujda/Angads zone

5 DISCUSSION

The integration of geophysical data, including GGM+ gravity and aeromagnetics, with thermal measurements and hydrogeochemical analyses, allows for a regional synthesis of the mechanisms governing the geothermal potential of Northeastern Morocco. Although each zone exhibits local specificities, the results highlight the coexistence of two distinct types of geothermal systems, both fundamentally controlled by regional crustal thinning. The common origin of the thermal anomalies observed throughout the region is intrinsically linked to

the geodynamic setting of lithospheric extension along the Morocco Hot Line (MHL) and the back-arc extension associated with the Alboran subduction system. Gravimetric analysis and Moho depth estimates of 20–30 km corroborate an upwelling of the asthenospheric mantle1111. This upwelling induces a general elevation of the basal heat flow above 80 mW/m^2, acting as a regional thermal engine. However, the mode of heat transfer to the surface differs radically between the Atlasic domain in the south and the Rif domain in the north.

The southern zones, comprising Berkane/Fezouane, Oujda/Angads, and Ain Goutitir/Taourirt, correspond to an Atlasic sedimentary conductive-advective model. In this intra-cratonic basin environment, the system is dominated by a deep aquifer composed of Liassic limestones and dolomites. This reservoir forms synclinal or graben structures trapped between Paleozoic horsts and is thermally insulated by a thick impermeable cover of Miocene marls and clays, which allows for the conservation of heat acquired at depth. Isotopic data indicate that meteoric recharge occurs on the high reliefs of the Beni Snassen and High Plateaus, where waters are cold and exhibit a Ca-HCO_3 facies. These waters infiltrate towards the basin centers, reaching depths exceeding 1500–2000 m, where they are heated primarily by conduction under a geothermal gradient of 30–45 °C/km. The ascent of these hot fluids to the surface is subsequently controlled by advection along the bounding faults of the horsts, such as the Fezouane or Ben Kachour faults. These structures act as vertical drains, allowing waters to emerge rapidly with temperatures of 30 to 54°C and evolved facies, ranging from Na-Cl to Ca-SO_4 depending on interactions with Triassic evaporites.

In contrast, the northern zones of Gourougou/Driouch and Arekman/Ras El Ma are characterized by a Rifain magmatic convective model. This high-enthalpy system is controlled by recent volcanism and active tectonics. Unlike the Atlasic model, the heat source here is not solely the basal flux but the presence of shallow magmatic intrusions linked to the Plio-Quaternary Gourougou volcanic complex. This magmatic influence explains the exceptional geothermal gradients (>80 °C/km) and heat flow densities reaching 120 mW/m^2. The reservoir architecture is complex, consisting of a fractured medium that includes the metamorphic basement (Temsamane schists), volcanic tuffs, and Mesozoic sediments. Heat transfer is dominated by vigorous hydrothermal convection. The presence of free gases (CO2, N2) with mantle isotopic signatures (3He) and high Radon concentrations provides evidence of very high permeability conduits connecting the surface to deep crustal zones. Furthermore, the high mineralization (Na-Cl facies) and coastal position suggest possible mixing with seawater or the dissolution of Triassic diapirs, processes that are favored by active tectonic extension which maintains open fracture networks.

The fundamental distinction between these two models lies in the heat transfer mechanism and the nature of permeability. The Atlasic system functions as a passive sedimentary basin system heated by burial, whereas the Rif system operates as an active magmatic system driven by intrusions and convection. This duality implies distinct exploration strategies: future efforts should target deep structural traps in the south for direct use applications, while targeting fault intersections and magmatic anomalies in the north for power generation potential.

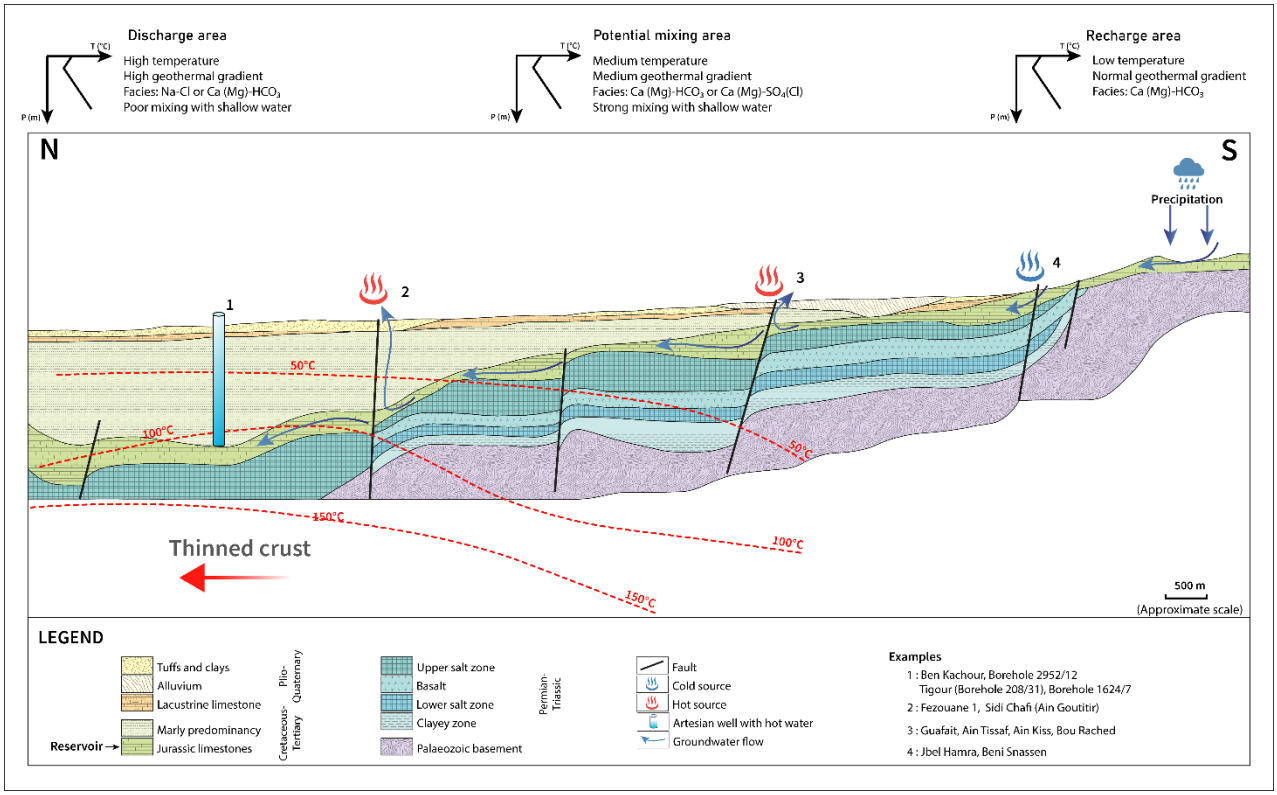


Figure 22. Conceptual model of the Atlasic Domain in Northeastern Morocco: Relationship between hydrodynamics, temperature, chemistry, and topography (schematic cross-section).

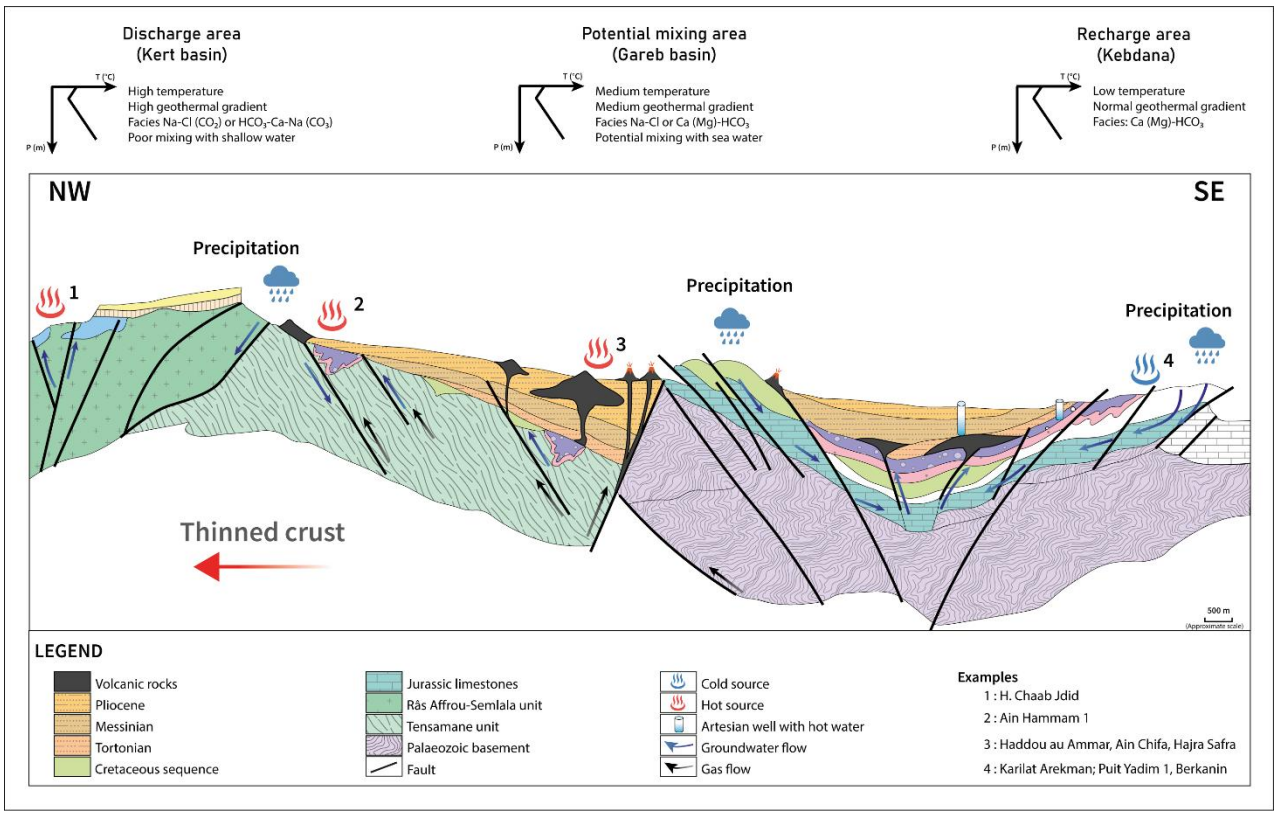


Figure 23: Conceptual model of the Pre-Rif Domain in Northeastern Morocco: Relationship between hydrodynamics, temperature, chemistry, and topography (schematic cross-section).

6 CONCLUSION

This study provides a comprehensive and updated conceptual understanding of the geothermal system in Northeastern Morocco, achieved through the rigorous integration of satellite gravity data (GGM+), spectral analysis of aeromagnetic data, borehole thermal profiling, and detailed hydrogeochemical investigations.

The multi-disciplinary approach has revealed that the thermal regime of the region is fundamentally controlled by the geodynamic setting of the Morocco Hot Line (MHL). The structural analysis, supported by GGM+ lineament extraction and Curie Point Depth estimates, confirms significant crustal thinning (Moho depths of 20–22 km) and the presence of deep-seated NE-SW faults that facilitate the ascent of heat and fluids from the mantle to the surface.

Based on these structural and thermal constraints, we have defined two distinct geothermal play types governing the region's potential:

- The Atlasic Sedimentary System (South): Characterized by a conductive-advective regime within deep Liassic carbonate reservoirs (e.g., Berkane, Oujda). This system is driven by a high regional background heat flow and deep circulation, resulting in medium-enthalpy resources (75–100°C) ideal for direct applications.

- The Rifain Magmatic-Convective System (North): Validated by the presence of magmatic gas signatures (^3He) and high radon concentrations in the Gourougou and Arekman zones. This system is driven by shallow magmatic intrusions and active extensional tectonics, creating a high-enthalpy convective environment.

Implications for Development:

The convergence of geophysical, thermal, and geochemical evidence unequivocally demonstrates the high power potential of Northeastern Morocco. The estimated reservoir temperatures, reaching 180–185°C in the northern volcanic province, confirm that this zone is highly suitable for electricity generation using Binary Cycle technology. Simultaneously, the extensive sedimentary reservoirs in the south offer a sustainable and robust resource for large-scale direct uses, particularly in agriculture (greenhouse heating), aquaculture, and balneotherapy.

In conclusion, Northeastern Morocco stands out as a premier target for geothermal development. The conceptual models proposed in this work provide a solid framework to reduce exploration risks and guide future drilling campaigns, positioning the region as a key contributor to the national renewable energy mix.

REFERENCES

Alsac, A., Cornet, G., Destombes, T. P., Hentinger, R., & Lavigne, J. (1969). *Etude géothermique du Maroc oriental*.

Barkaoui, A. E., Zarhloule, Y., Varbanov, P. S., & Klemeš, J. J. (2017). Geothermal power potential assessment in North Eastern Morocco. *Chemical Engineering Transactions*, *61*, 1627–1632. https://doi.org/10.3303/CET1761269

Barkaoui, A. E., Zarhloule, Y., Verdoya, M., Pasquale, V., & Lahrach, H. (2014). Progress in understanding the geothermal sedimentary basins in northeastern Morocco. *Journal of African Earth Sciences*, *97*, 1–8. https://doi.org/10.1016/j.jafrearsci.2014.04.036

Boumehdi, M., Hahou, Y., Amrouch, K., Berkat, N. E., Carneiro, J., Correia, A., & Sadki, O. (2025). New assessment of geothermal resources in Morocco: Evaluation of the curie point depth method using magnetic data for geothermal gradient and heat flow estimation. *Scientific African*, *28*, e02726. https://doi.org/10.1016/j.sciaf.2025.e02726

Cidu, R., & Bahaj, S. (2000). Geochemistry of thermal waters from Morocco. *Geothermics*, *29*(3), 407–430. https://doi.org/10.1016/S0375-6505(00)00007-9

de Lamotte, D. F., Leturmy, P., Missenard, Y., Khomsi, S., Ruiz, G., Saddiqi, O., Guillocheau, F., & Michard, A. (2009). Mesozoic and Cenozoic vertical movements in the Atlas system (Algeria, Morocco, Tunisia): An overview. *Tectonophysics*, *475*(1), 9–28. https://doi.org/10.1016/j.tecto.2008.10.024

Díaz, J., Gil, A., Carbonell, R., Gallart, J., & Harnafi, M. (2016). Constraining the crustal root geometry beneath Northern Morocco. *Tectonophysics*, *689*, 14–24. https://doi.org/10.1016/j.tecto.2015.12.009

El Bakkali, S., Gourgaud, A., Bourdier, J.-L., Bellon, H., & Gundogdu, N. (1998). Post-collision neogene volcanism of the Eastern Rif (Morocco): magmatic evolution through time. *Lithos*, *45*(1–4), 523–543. https://doi.org/10.1016/S0024-4937(98)00048-6

Fournier, R. O., & Potter, R. W. (1979). Magnesium correction to the Na□K□Ca chemical geothermometer. *Geochimica et Cosmochimica Acta*, *43*(9), 1543–1550. https://doi.org/10.1016/0016-7037(79)90147-9

Fournier, R. O., & Truesdell, A. H. (1973). An empirical Na□K□Ca geothermometer for natural waters. *Geochimica et Cosmochimica Acta*, *37*(5), 1255–1275. https://doi.org/10.1016/0016-7037(73)90060-4

Fullea, J., Fernàndez, M., & Zeyen, H. (2006). Lithospheric structure in the Atlantic-Mediterranean transition zone (southern Spain, northern Morocco): A simple approach from regional elevation and geoid data. *Comptes Rendus - Geoscience*, *338*(1–2), 140–151. https://doi.org/10.1016/j.crte.2005.11.004

Fullea, J., Fernàndez, M., Zeyen, H., & Vergés, J. (2007). A rapid method to map the crustal and lithospheric thickness using elevation, geoid anomaly and thermal analysis. Application to the Gibraltar Arc System, Atlas Mountains and adjacent zones. *Tectonophysics*, *430*(1–4), 97–117. https://doi.org/10.1016/j.tecto.2006.11.003

Giggenbach, W. F. (1988). Geothermal solute equilibria. Derivation of Na-K-Mg-Ca geoindicators. *Geochimica et Cosmochimica Acta*, *52*(12), 2749–2765. https://doi.org/10.1016/0016-7037(88)90143-3

Gil, A., Gallart, J., Diaz, J., Carbonell, R., Torne, M., Levander, A., & Harnafi, M. (2014). Crustal structure beneath the Rif Cordillera, North Morocco, from the RIFSIS wide-angle reflection seismic experiment. *Geochemistry, Geophysics, Geosystems*, *15*(12), 4712–4733. https://doi.org/10.1002/2014GC005485

Haffou, F. Z., Ouzzaouit, L. A., Qarbous, A. A., & Boudad, L. L. (2024). Assessment and Modeling of Geothermal Potential in Northeastern Morocco. *Iraqi Geological Journal*, *57*(1D), 9–20. https://doi.org/10.46717/igj.57.1D.2ms-2024-4-12

Helgeson, H. C., Brown, T. H., Nigrini, A., & Jones, T. A. (1970). Calculation of mass transfer in geochemical processes involving aqueous solutions. *Geochimica et Cosmochimica Acta*, *34*(5), 569–592. https://doi.org/10.1016/0016-7037(70)90017-7

Hirt, C., Claessens, S., Fecher, T., Kuhn, M., Pail, R., & Rexer, M. (2013). New ultrahigh-resolution picture of Earth's gravity field. *Geophysical Research Letters*, *40*(16), 4279–4283. https://doi.org/10.1002/grl.50838

Jacobshagen, V. (1992). Major fracture zones of Morocco: The South Atlas and the Transalboran fault systems. *Geologische Rundschau*, *81*(1), 185–197. https://doi.org/10.1007/BF01764548

Lee, R. W., & Strickland, D. J. (1988). Geochemistry of groundwater in tertiary and cretaceous sediments of the southeastern Coastal Plain in eastern Georgia, South Carolina, and southeastern North Carolina. *Water Resources Research*, *24*(2), 291–303. https://doi.org/10.1029/WR024i002p00291

Li, Q., Palomeras, I., & Meng, X. (2021). Lithospheric structure beneath southern Iberia and northern Morocco constrained by 3D Kirchhoff-approximate GRT imaging. *Journal of Geophysics and Engineering*, *18*(2), 268–281. https://doi.org/10.1093/jge/gxab012

Mancilla, F. de L., & Diaz, J. (2015). High resolution Moho topography map beneath Iberia and Northern Morocco from receiver function analysis. *Tectonophysics*, *663*, 203–211. https://doi.org/10.1016/j.tecto.2015.06.017

Missenard, Y., Zeyen, H., Frizon De Lamotte, D., Leturmy, P., Petit, C., Sebrier, M., Missenard, Y., Zeyen, H., Frizon De Lamotte, D., Leturmy, P., Petit, C., Sébrier, M., & Saddiqi, O. (2006). Crustal versus asthenospheric origin of the relief of the Atlas Mountains of Morocco. Crustal versus asthenospheric origin of relief of the Atlas Mountains of Morocco. *Journal of Geophysical Research*, *111*, 3401. https://doi.org/10.1029/2005JB003708ï

Nordstrom, D. K., & Jenne, E. A. (1977). Fluorite solubility equilibria in selected geothermal waters. *Geochimica et Cosmochimica Acta*, *41*(2), 175–188. https://doi.org/10.1016/0016-7037(77)90224-1

Ouzzaouit, L. A., EL Ouassif, B., Idri, A., Qarbous, A., Barich, A., Weisenberger, T. B., & Boudad, L. (2023). Geothermal flow in Northern Morocco: A machine learning approach. *Journal of African Earth Sciences*, *205*. https://doi.org/10.1016/j.jafrearsci.2023.104995

Platt, J. P., Behr, W. M., Johanesen, K., & Williams, J. R. (2013). The Betic-Rif Arc and Its Orogenic Hinterland: A Review. *Annual Review of Earth and Planetary Sciences*, *41*(1), 313–357. https://doi.org/10.1146/annurev-earth-050212-123951

Reed, M., & Spycher, N. (1984). Calculation of pH and mineral equilibria in hydrothermal waters with application to geothermometry and studies of boiling and dilution. *Geochimica et Cosmochimica Acta*, *48*(7), 1479–1492. https://doi.org/10.1016/0016-7037(84)90404-6

Rimi, A. (1999). Mantle heat flow and geotherms for the main geologic domains in Morocco. In *Int Journ Earth Sciences* (Vol. 88). Springer-Verlag.

Rimi, A., & Lucazeau, F. (1987). Heat flow density measurements in northern Morocco. *Journal of African Earth Sciences (1983)*, *6*(6), 835–843. https://doi.org/10.1016/0899-5362(87)90041-8

Rimi, A., Zarhloule, Y., Barkaoui, A. E., Correia, A., Carneiro, J., Verdoya, M., & Lucazeau, F. (2012). Towards a de-carbonized energy system in north-eastern Morocco: Prospective geothermal resource. *Renewable and Sustainable Energy Reviews*, *16*(4), 2207–2216. https://doi.org/10.1016/j.rser.2011.12.008

Takherist, D., & Lesquer, A. (1989). Mise en évidence d'importantes variations régionales du flux de chaleur en Algérie. *Canadian Journal of Earth Sciences*, *26*(4), 615–626. https://doi.org/10.1139/e89-053

Truesdell, A.H.; 1976. Summary of Section III. Geochemical techniques in exploration. Proceedings of the 2nd United .Nations Symposium on the Development and Use of Geothermal Resources, San Francisco: 53-79.

van Hinsbergen, D. J. J., Vissers, R. L. M., & Spakman, W. (2014). Origin and consequences of western Mediterranean subduction, rollback, and slab segmentation. *Tectonics*, *33*(4), 393–419. https://doi.org/10.1002/2013TC003349

Winckel, A., Marlin, C., Dever, L., Morel, J.-L., Morabiti, K., Makhlouf, M. B., & Chalouan, A. (2002). Apport des isotopes stables dans l'estimation des altitudes de recharge de sources thermales du Maroc. *Comptes Rendus. Géoscience*, *334*(7), 469–474. https://doi.org/10.1016/S1631-0713(02)01764-9

Zarhloule, Y. (2004). Le gradient géothermique profond du Maroc : détermination et cartographie. *Bulletin de l'Institut Scientifique*, *26*, 11–25.

Zarhloule, Y., Rimi, A., Boughriba, M., Barkaoui, A. E., & Lahrach, A. (2015). *The Geothermal Research in Morocco: History of 40 Years*.

Zarhloule, Y., Rimi, A., Boughriba, M., Verdoya, M., Correia, A., Carneiro, J., & Lahrach, A. (2007). *La province géothermique du Maroc Nord Oriental*.